

## X-RAY EMISSION FROM THE HOST CLUSTERS OF POWERFUL AGN

Patrick B. Hall

Steward Observatory, University of Arizona, Tucson, AZ 85721

E-Mail: pathall@as.arizona.edu

Erica Ellingson

Center for Astrophysics and Space Astronomy, CB 391, University of Colorado,  
Boulder, CO 80309

and

Richard F. Green

National Optical Astronomy Observatories<sup>1</sup>, Tucson, AZ 85726-6732

### ABSTRACT

We report the detection of X-ray emission from the host cluster of the unusual radio-quiet quasar H 1821+643 using the *ROSAT* HRI, and the non-detection of X-ray emission from the host cluster of the radio-loud quasar 3C 206 ( $3\sigma$  upper limit of  $1.63 \cdot 10^{44}$  ergs  $s^{-1}$ ) using the *EINSTEIN* HRI. The host cluster of H 1821+643 is one of the most X-ray luminous clusters known, with a rest-frame 0.1-2.4 keV luminosity of  $3.74 \pm 0.57 h_{50}^{-2} \cdot 10^{45}$  ergs  $s^{-1}$ , 38% of which is from a barely resolved cooling flow component. The cluster emission complicates interpretation of previous X-ray spectra of this field. In particular, the observed Fe  $K\alpha$  emission can probably be attributed entirely to the cluster and either the quasar is relatively X-ray quiet for its optical luminosity or the cluster has a relatively low temperature for its luminosity.

We combine these data with the recent detection of X-ray emission from the host cluster of the ‘buried’ radio-quiet quasar IRAS 09104+4109 (Fabian & Crawford 1995), our previous upper limits for the host clusters of two  $z \sim 0.7$  radio-loud quasars, and literature data on FR II radio galaxies. We compare this dataset to the predictions of three models for the presence and evolution of powerful AGN in clusters: the low-velocity-dispersion model, the low-ICM-density model, and the cooling flow model.

Neither the low-ICM-density model nor the cooling flow model can explain all the observations. We suggest that strong interactions with gas-containing galaxies may be the only mechanism needed to explain the presence and evolution of powerful AGN

---

<sup>1</sup>The National Optical Astronomy Observatories are operated by the Association of Universities for Research in Astronomy under Cooperative Agreement with the National Science Foundation.

in clusters, a scenario consistent with the far-IR and optical properties of the host galaxies studied here, all of which show some evidence for past interactions. However, the cooling flow model cannot be ruled out for at least some objects, and it is likely that both processes are at work in creating and fueling powerful AGN in clusters. Each scenario makes testable predictions for future X-ray and optical observations which can test the relative importance of each process.

*Subject headings:* Clusters of Galaxies, Quasi-Stellar Objects, Active Galaxies, X-ray Sources, White Dwarfs, Planetary Nebulae

## 1. Introduction

The association of quasars with galaxies at similar redshifts allows one to use quasars as signposts for locating galaxies and galaxy clusters at high redshift. Although radio-quiet quasars (RQQs) are very rarely found in clusters at  $z \lesssim 0.7$ , a significant fraction of radio-loud quasars (RLQs) with  $0.4 < z < 0.7$  are located in clusters of galaxies (e.g., Yee & Green 1987 (YG87), Ellingson, Yee & Green 1991 (EYG91), Ellingson & Yee 1994). The population of quasars located in such rich clusters is seen to evolve 5–6 times faster than their counterparts in poor environments (EYG91, Yee & Ellingson 1993): at  $z \lesssim 0.4$  RLQs are almost never found in rich clusters, at  $z \sim 0.4-0.55$  only faint RLQs can be found in them, and at  $z \gtrsim 0.55$  both luminous and faint RLQs are found there (cf. Figure 1 of Yee & Ellingson 1993). This evolution can be extrapolated to include the very faint optical AGN activity seen in some radio galaxies in low-redshift rich clusters (e.g. DeRobertis & Yee 1990). The environments of the population of Fanaroff-Riley class II (FR II) ‘classical double’ powerful radio galaxies (PRGs) evolve with redshift as well (Prestage & Peacock 1988, Yates, Miller & Peacock 1989, Hill & Lilly 1991, Allington-Smith et al. 1993). RLQs also have FR II morphologies, and in the unification model (Antonucci 1993) PRGs and RLQs are the same class of objects seen at different orientations, in which case their large-scale environments should be statistically identical. One scenario which can explain these observations is that the physical conditions in RLQ and PRG host cluster cores have undergone substantial changes which have caused the high- $z$  FR II RLQs and PRGs in clusters to fade at optical wavelengths on a dynamical time scale and evolve into low- $z$  optically faint FR I radio galaxies.

In the context of this evolution the results of Tsai & Buote (1996) are quite interesting. They conclude from hydrodynamical simulations that in an  $\Omega=1$  CDM universe the formation rate of clusters from (unvirialized) background matter was large at  $z \gtrsim 0.6$ , but dropped off sharply at  $z \sim 0.6$  and remained constant and small at  $z < 0.6$ , where new clusters form primarily by mergers of preexisting, virialized smaller clusters. This is very similar to the scenario suggested by Yee & Ellingson (1993) to explain the steep decline in the optical luminosities of RLQ population in rich clusters at  $z \lesssim 0.6$ . The RLQ luminosity function is consistent with a constant cluster birth rate providing a continual supply of RLQ formation sites at  $z > 0.6$ , in agreement with the Tsai & Buote

simulations if clusters formed by mergers of preexisting subclusters are unfavorable sites for RLQ formation. This agreement is intriguing but possibly coincidental, as other simulations (Richstone, Loeb & Turner 1992, Cen & Ostriker 1994) yield different cluster formation rates with redshift.

Many mechanisms have been put forth as explanations for the quasar environment-evolution link: galaxy-galaxy interactions and mergers (Hutchings, Crampton & Campbell 1984), cooling flows (Fabian & Crawford 1990), and/or an intra-cluster medium (ICM) of different density at high redshift (Stoche & Perrenod 1981, Barthel & Miley 1988). These different models have considerably different implications for X-ray observations of quasar host clusters, as discussed in Hall et al. (1995; hereafter Paper I) and in §3. We are imaging quasars known to lie in rich clusters with the *ROSAT* High Resolution Imager (HRI; Zombeck et al. 1990) to help discriminate among these scenarios for the evolution of powerful AGN in clusters and the role played by the ICM in that evolution. Paper I presented upper limits for the first two quasars we studied. In this paper we add new data on one lower-redshift quasar, archival data on another, and data from the literature on a third. We then discuss the data in comparison to FR II radio galaxy host clusters and optically and X-ray selected clusters. We restrict our discussion primarily to PRGs and quasars with unambiguous FR II morphologies believed to be located at the centers of their host clusters. Unless otherwise noted, we take  $H_0=50 \text{ h}_{50} \text{ km s}^{-1} \text{ Mpc}^{-1}$ ,  $q_0=1/2$ , and  $\Lambda=0$ .

## 2. Observations and Analysis

Table 1 details the observations and results discussed in this paper, Paper I, and Crawford & Fabian (1995). The three objects newly added to our sample are discussed in detail in this section.

### 2.1. IRAS 09104+4109

IRAS 09104+4109 is a very IR-luminous ‘buried’ radio-quiet quasar (Hines & Wills 1993; HW93) at the center of a rich, flattened cluster at  $z=0.442$  (Kleinmann et al. 1988). It is a radio source intermediate between FR I and FR II in radio power and morphology (HW93). HW93 show that IRAS 09104+4109 is powered by a hidden AGN based on the detection of broad Mg II  $\lambda 2798$  and strong wavelength-dependent polarization. We classify IRAS 09104+4109 as a RQQ based on its k-corrected 5 GHz to (estimated) unobscured B luminosity ratio  $R^*$  (Stoche et al. 1992). Using data from HW93, we find  $R^*=0.89\text{--}4.27$ , placing it at the high end of the range found for RQQs. Also, its position in the O[III]- $P_{5\text{GHz}}$  plane (Rawlings 1994) clearly shows it to be a RQQ, albeit an extreme one (similar to H 1821+643), even after accounting for its steep radio spectral slope and correcting its large O[III] luminosity for non-nuclear emission (Crawford & Vanderriest 1996). We estimated the richness  $B_{\text{gq}}$  of the host cluster CL 09104+4109 by using data from Kleinmann et al. (1988) to find  $N_{0.5}$  (Bahcall 1981) and then converting to  $B_{\text{gq}}$  using the empirical relation

$B_{\text{gq}}=34 \times N_{0.5}$  (Hill & Lilly 1991). We find  $B_{\text{gq}}=1210_{-269}^{+316}$ , equivalent to Abell richness 2. The host galaxy is a cD possibly in the midst of cannibalizing several smaller galaxies (Soifer et al. 1996).

CL 09104+4109 has been detected by the *ROSAT* HRI (Fabian & Crawford 1995; hereafter FC95; see also Crawford & Vanderriest 1996). It is one of the most X-ray luminous clusters known and shows evidence for a cooling flow in the form of an excess central emission component above the best-fit King model. An apparent deficit in the central X-ray emission is also observed, possibly caused by HI absorption in a cooling flow, or by displacement of the ICM by the radio jets or a mass outflow from the center of the host galaxy (Crawford & Vanderriest 1996). FC95 calculate  $L_X=2.9 \pm 0.25 \times 10^{45}$  ergs  $s^{-1}$  in the observed *ROSAT* band, and  $kT=11.4_{-3.2}^{+\infty}$  keV from a fit to an ASCA spectrum of the object. Using a  $kT=11.4$  keV thermal brehmsstrahlung spectrum redshifted to  $z=0.442$ , we calculate a rest-frame 0.1–2.4 keV luminosity  $3.03 \pm 0.26 \times 10^{45}$  ergs  $s^{-1}$ . Although the quasar and its cD host are at the center of the X-ray emission, they may not lie at the optical center of the cluster (Kleinmann et al. 1988).

## 2.2. 3C 206

The first observation we present is of the radio-loud quasar (RLQ) 3C 206 ( $z=0.1976$ ). 3C 206 resides in a flattened cluster of Abell richness class 1 which has a lower velocity dispersion than is typical for such clusters (Ellingson et al. 1989). The cluster (which we designate CL 3C 206) is very centrally concentrated, with a best-fit optical core radius of 35 kpc (Ellingson et al. 1989). 3C 206 is unusual in that it is the only radio-loud quasar at  $z < 0.4$  known to reside in a cluster of Abell richness 0 or greater. The host galaxy of 3C 206 is an elliptical in the approximate optical center of the host cluster, but the galaxy is  $\gtrsim 1$  mag fainter than expected for a first-rank cluster galaxy (Ellingson et al. 1989, Hutchings 1987). The host galaxy is slightly redder than a typical RLQ host galaxy but slightly bluer than a normal elliptical (Ellingson et al. 1989).

### 2.2.1. Analysis of *EINSTEIN* HRI Observations of 3C 206

Our ‘observation’ of 3C 206 consists of a 61 ksec archival *EINSTEIN* High Resolution Imager (HRI) image. No extended emission is obvious in the image. Since our non-detection data analysis techniques were discussed in detail in Paper I, we give only an overview here. Our modeling requires binned radial profiles for the object, the HRI Point Response Function (PRF), and for PRF-convolved  $\beta=2/3$  King model clusters of  $r_{\text{core}}=125$  and 250 kpc at the quasar redshift for several different cosmologies. After background subtraction, the PRF was normalized to the object counts in the innermost bin and subtracted, leaving a radial profile consisting of any excess counts above the profile expected for an object of the observed central intensity. The object’s radial profile, the fitted PRF and background, and the PRF subtracted (but not background subtracted) residual profile are plotted in Figure 1. The residual is exaggerated in this log-log plot; note that

the apparent excess emission is of the same scale as the PRF and that the residual is negative between 15-40'', where cluster emission should be most prominent. Since the PRF fit is sufficient, we derive a cts s<sup>-1</sup> value for a 3σ upper limit cluster as described in Paper I. This upper limit on cluster cts s<sup>-1</sup> within 8' was corrected for deadtime and vignetting through comparison with the *EINSTEIN* HRI source catalog (available through the Einstein On-Line Service of the SAO). We measured the counts of the quasar and the next brightest source in the 3C 206 field in exactly the same manner as the HRI source catalog. and found the archive count rates to still be a factor 1.112 higher than ours. Although this deadtime plus vignetting correction factor is somewhat higher than might be expected, we adopt it to be conservative.

To convert our limit from cts s<sup>-1</sup> to L<sub>X</sub>, we first convert to the emitted flux in the *EINSTEIN* passband corrected for Galactic absorption of log N<sub>H</sub>=20.75 (Elvis, Lockman & Wilkes 1989). We assume a Raymond & Smith (1977) plasma spectrum with temperature from

$$\beta = \mu m_p \sigma_v^2 / kT \quad (1)$$

where μ is the mean molecular weight of the cluster gas (0.63 for solar abundance) and σ<sub>v</sub> is the cluster velocity dispersion. Assuming β=2/3 gives kT=2.5±1.1 keV using the observed σ<sub>v</sub>=500±110 km s<sup>-1</sup>. Using the *EINSTEIN* Users Manual (Harris 1984), we find a conversion factor 1.3 10<sup>-13</sup> ergs cm<sup>-2</sup> count<sup>-1</sup> for this N(HI) and kT.

For intercomparison of our targets we convert to the rest-frame *ROSAT* passband (0.1-2.4 keV). Conversions were calculated using redshifted thermal brehmsstrahlung spectra and the effective areas as a function of energy for the *EINSTEIN* and *ROSAT* HRIs given in HH86 and David et al. (1995). Next we convert this rest-frame 0.1-2.4 keV band flux F to a luminosity L<sub>X</sub> using F=L<sub>X</sub>/4πD<sub>L</sub><sup>2</sup>, where D<sub>L</sub> is the quasar's luminosity distance in the assumed cosmology:

$$D_L = \frac{2cz}{H_o(G+1)} \left( 1 + \frac{z}{G+1} \right) \quad (2)$$

where G=√(1+2zq<sub>o</sub>) (Schmidt & Green 1986). (Note that the equations for D<sub>L</sub> given in Paper I are incorrect.) Finally, we correct the cluster luminosity for emission beyond r=8'.

The resulting upper limits, for different cosmologies and core radii, are given in Table 2. For kT=2.5 keV and r<sub>core</sub>=125 kpc our CL 3C 206 3σ upper limit is 1.63 10<sup>44</sup> ergs s<sup>-1</sup>. Also given in Table 2 are our upper limits from Paper I, now corrected to the rest-frame 0.1-2.4 keV band.

### 2.3. H 1821+643

H 1821+643 (z=0.297) is an IR-luminous X-ray selected radio-quiet quasar (RQQ) residing in a giant elliptical galaxy in a rich (Abell richness class ~2) cluster at low redshift. (H 1821+643 and IRAS 09104+4109 have the richest quasar host clusters known at any redshift.) H 1821+643

has been detected and studied in the radio despite being radio-quiet (Lacy, Rawlings & Hill 1992, Blundell & Lacy 1995, Papadopoulos et al. 1995, Blundell et al. 1996). It has a core, a lobe, and two small jets (Blundell & Lacy 1995, Blundell et al. 1996). We calculate  $\sigma_v=1046\pm108$  km s<sup>-1</sup> for CL 1821+643 (in its rest frame) using 26 members from Schneider et al. (1992) and Le Brun, Bergeron & Boissé (1995). The host galaxy is bright, large, red, and featureless, but slightly asymmetrical and offset from the nucleus by 1-2'' (Hutchings & Neff 1991b). All the galaxy's measured parameters are consistent with it being a cD at the center of the cluster.

### 2.3.1. Analysis of ROSAT HRI Observations of H 1821+643

Our ROSAT HRI observation of H 1821+643 is shown in Figure 2, binned into 1'' pixels. Both the quasar and the nearby white dwarf central star of the planetary nebula Kohoutek 1-16 (K1-16) are easily detected, along with obvious extended emission from the quasar host cluster. The X-ray emission from K1-16 shows no signs of being resolved on our HRI image. Isophote fitting from r=10''–70'' on an adaptively smoothed (Worrall, Birkinshaw & Cameron 1995) image showed that the cluster has an ellipticity of ~0.1 at all radii. The cluster isophotes' center is, within the errors, the same as the quasar position for all r<70''. To decrease the FWHM and ellipticity of the PRF in our data, we subdivided the image by exposure time, centroided, and restacked (cf. Morse 1994). We also added a 1460 sec archival HRI image of the field at this stage. We then extracted the quasar and white dwarf radial profiles using annuli of 1'' width on the corrected, unbinned, unsmoothed HRI image, excluding data within r=22''.5 of all objects detected by the standard processing, and fitted the radial profile of emission surrounding the quasar.

### 2.3.2. H 1821+643 Radial Profile

We initially assume a three-component radial profile: a constant background, a ROSAT HRI PRF, and a King surface brightness cluster ( $S(r) \propto [1 + (r/r_{\text{core}})^2]^{-(3\beta-0.5)}$ ) convolved with the ROSAT HRI PRF. (Because of the complexity in fitting a non-analytic PRF-convolved King profile to the data, we fit a simple King profile instead; simulations indicate <5% systematic error in this procedure, which we account for in our results.) The parameters in our model are the background level, the normalization, core radius, and  $\beta$  of the King profile, the PRF normalization, the widths  $\sigma_1$  and  $\sigma_2$  of the two gaussians that comprise the PRF (see Paper I and David et al. (1995); hereafter D95), and the relative normalizations of the PRF gaussians. We kept the normalization and scale length of the exponential PRF component fixed at the standard values in all models.

We used NFIT1D in IRAF<sup>2</sup> to fit our model to the observed radial profile. We used  $\beta=2/3$

---

<sup>2</sup>The Image Reduction and Analysis Facility is distributed by National Optical Astronomy Observatories, operated by the Association of Universities for Research in Astronomy, Inc., under contract to the National Science Foundation.

and the standard normalization of the two PRF gaussians; all other parameters were allowed to vary. The solution (plotted in Figure 3a) was good (reduced  $\chi^2=0.8612$ ) but it gave a value of  $\sigma_2=4''.58\pm 0''.05$ , noticeably above the maximum of  $4''.1$  measured for long PRF characterization observations (David et al. 1995). We attempted to produce an adequate fit more in line with the known PRF properties by allowing the all the parameters to vary, but no fit gave a smaller  $\sigma_2$ .

To see if our broad PRF result was robust, we fitted the PRF of the white dwarf using data within  $r=23''$ . The best fit (reduced  $\chi^2=0.698$ ) had  $\sigma_1=2''.03\pm 0''.18$  and  $\sigma_2=4''.08\pm 0''.20$ , consistent with the standard values and the range of observed values (D95). So, either the PRF in our image is best given by the fit to the quasar, not the white dwarf, and is slightly broader than measured in the PRF characterization observations, or the PRF is best given by the fit to the white dwarf and there is a barely resolved component to the cluster emission which broadens the fitted quasar radial profile. Such a component would most likely be due to a cooling flow.

To test the hypothesis that a single King profile is inadequate to describe the cluster emission, we fitted a simple gaussian along with a point source and a  $\beta=2/3$  King profile. The best fit (plotted in Figure 3b) was a considerable improvement (F-test probability  $<0.5\%$  of occurring by chance) and had  $\sigma_2=2''.34\pm 0''.04$  and  $\sigma_2=3''.91\pm 0''.20$ , smaller than in the fit without the extra gaussian and consistent with the WD fit and the range observed in PRF characterization observations. However, the amplitude of the gaussian component is constrained to only  $\pm 32\%$ .

Thus the total cluster emission is better described by a King profile plus a barely resolved component than a King model alone, but the amplitude of the barely resolved component is considerably uncertain. As a check, we fitted a King model and gaussian to the original, uncorrected image, and found that the parameters for both components were identical within the errors to the values determined from the corrected image. The King component of the cluster's total flux is  $3523\pm 498$  counts. The best-fit additional gaussian component has  $2139\pm 713$  counts, for a total of  $5662\pm 870$  cluster counts, integrated to infinity.

### 2.3.3. CL 1821+643 Physical Parameters

Several steps must be taken to convert from  $\text{cts s}^{-1}$  to  $L_X$ . We take Galactic  $\log N(\text{HI})=20.58$  (Lockman & Savage 1995) and assume a Raymond-Smith spectrum with observed  $kT=5$  keV, the highest value tabulated in D95; a higher value would increase the estimated  $L_X$  only a little, since *ROSAT* has little effective area above 2 keV. We find the energy-to-counts conversion factor as described in Paper I and divide this factor (0.223) into our  $\text{cts s}^{-1}$  limit to obtain the energy flux in units of  $10^{-11} \text{ ergs cm}^{-2} \text{ s}^{-1}$ . We then convert to  $L_X$  in the rest-frame 0.1-2.4 keV band. We measure a rest-frame 0.1-2.4 keV luminosity of  $3.74\pm 0.57 h_{50}^{-2} 10^{45} \text{ ergs s}^{-1}$  for CL 1821+643 with  $2.33\pm 0.33$  and  $1.41\pm 0.47 h_{50}^{-2} 10^{45} \text{ ergs s}^{-1}$  from the King model and cooling flow components respectively. The values of  $L_X$  for different cosmologies are tabulated in Table 2. This luminous cluster complicates the interpretation of previous X-ray observations of this field (Appendix A).

The detection of ICM X-ray emission allows us to calculate the central electron number density  $n_{e,0}$  of the cluster if the emission follows a King model, and to put a lower limit on it in the case of a cooling flow. For  $\beta=2/3$ , equation (3) of Henry & Henriksen (1986; HH86) becomes:

$$I(0; E_1, E_2) = 1.91 \times 10^{-3} n_{e,0}^2 r_c \sqrt{kT} [\gamma(0.7, E_1/kT) - \gamma(0.7, E_2/kT)] \text{ ergs s}^{-1} \text{ cm}^{-2} \text{ sr}^{-1} \quad (3)$$

where  $r_c$  is the cluster core radius in kpc,  $n_{e,0}$  is the central electron number density of the cluster in  $\text{cm}^{-3}$ ,  $kT$  is the cluster temperature in keV, and  $\gamma(a,z)$  is the incomplete gamma function  $\int_z^\infty x^{a-1} e^{-x} dx$ . (The order of the gamma function terms is incorrectly reversed in HH86).  $I(0; E_1, E_2)$  is the cluster's central X-ray surface brightness (at the cluster) in the band  $E_1$  to  $E_2$ , and  $E_1$  and  $E_2$  are the energies (in keV) corresponding to the lower and upper limits, respectively, of the instrumental passband *at the object's redshift*. For *ROSAT*,  $E_1=0.1(1+z)$  keV and  $E_2=2.4(1+z)$  keV.  $I(0; E_1, E_2)$  can be related to  $I_{\text{obs}}$ , the observed central surface brightness in the  $(E_1, E_2)$  band in  $\text{ergs cm}^{-2} \text{ s}^{-1} \text{ arcsec}^{-2}$  as follows (see also Birkinshaw & Worrall 1993). For  $\beta=2/3$ , the total cluster X-ray luminosity in the  $(E_1, E_2)$  band is easily found by integrating the surface brightness either at the source or at the observer. Equating the two, we have:

$$L_X(E_1, E_2) = I(0; E_1, E_2) 4\pi 2\pi r_{\text{core}}^2 = I_{\text{obs}} 4\pi d_L^2 2\pi \theta_c^2 \quad (4)$$

where  $r_{\text{core}}$  and  $d_L$  are in cm and  $\theta_c$  is the angular size corresponding to  $r_{\text{core}}$  at the object's redshift. This yields

$$I(0; E_1, E_2) = I_{\text{obs}} d_L^2 \theta_c^2 / r_{\text{core}}^2 \quad (5)$$

Also, if the cluster  $T$  is unknown but  $\sigma_v$  is, we can use Eq. 1 for  $\beta=2/3$  to replace  $\sqrt{kT}$  in Eq. 3:

$$I(0; E_1, E_2) = 5.86 \times 10^{-6} n_{e,0}^2 r_c \sigma_v [\gamma(0.7, E_1/kT) - \gamma(0.7, E_2/kT)] \text{ ergs s}^{-1} \text{ cm}^{-2} \text{ sr}^{-1} \quad (6)$$

where  $\sigma_v$  is in  $\text{km s}^{-1}$ . For H 1821+643, we find  $n_{e,0}=0.015\pm 0.002 h_{50}^{1/2} \text{ cm}^{-3}$  for the King model component and a lower limit of  $n_{e,0}=0.081\pm 0.022 h_{50}^{1/2} \text{ cm}^{-3}$  for the cooling flow component using the central surface brightness of our gaussian fit. (Strictly speaking a deprojection analysis is required to calculate  $n_{e,0}$  in the case of a cooling flow, and the densities will still be underestimated because the central regions are unresolved, but our estimates should be accurate lower limits.)

With an estimate for  $n_{e,0}$ , we can estimate  $t_{\text{cool}}$ , the cooling time for gas in the center of the cluster, using equation (5.23) of Sarazin (1988):

$$t_{\text{cool}} = 2.89 \cdot 10^7 n_{e,0}^{-1} \sqrt{T} \text{ years} \quad (7)$$

where  $T$  (estimated from  $\sigma_v$  using Eq. 1 if necessary) is in keV,  $n_{e,0}$  is in  $\text{cm}^{-3}$ , and we have used the relation  $n_p=0.82n_{e,0}$  for completely ionized H-He gas. We find  $t_{\text{cool}} < 6.4 \pm 1.2 h_{50}^{-1/2} \text{ Gyr}$  (since  $n_{e,0} \propto h_{50}^{1/2}$ ), which is less than the age of the universe at  $z=0.297$ ,  $8.8 h_{50}^{-1} \text{ Gyr}$  ( $10.1 h_{50}^{-1} \text{ Gyr}$  for  $q_0=0$ ), for all reasonable  $H_0$ . Thus CL 1821+643 meets the standard criteria for the presence of a central cooling flow. The mass cooling rate  $\dot{M}_{\text{cool}}$  can be found from

$$L_{\text{cool}} = 2.4 \cdot 10^{43} T_{\text{keV}} \dot{M}_{\text{cool},100} \text{ ergs s}^{-1} \quad (8)$$



where  $L_{\text{cool}}$  is the total luminosity of the cooling gas,  $T_{\text{keV}}$  its initial temperature, and  $\dot{M}_{\text{cool},100}$  the mass deposition rate in  $100 h_{50}^{-2} M_{\odot} \text{ yr}^{-1}$  (Fabian et al. 1986). We find  $\dot{M}_{\text{cool}}=1120\pm 440 h_{50}^{-2} M_{\odot} \text{ yr}^{-1}$  for H 1821+643. This is likely a lower limit since we have not used the bolometric  $L_{\text{cool}}$ .

### 3. Discussion

#### 3.1. Physical Parameters of Quasar Host Clusters

Only five quasar host clusters have observations deep enough to put interesting limits on their X-ray emission. The two detections and three upper limits are listed in Table 2. We note that the three upper limits are for the host clusters of RLQs with  $P_{20\text{cm}} > 10^{26} \text{ W/Hz}$  and the detections are of the host clusters of two RQQs with  $P_{20\text{cm}} \sim 10^{25} \text{ W/Hz}$ , two of the richest quasar host clusters known at any redshift, which are two of the most X-ray luminous clusters known.

These two luminous RQQ host clusters have dense ICM (cf. Table 1, §2.3.3). For CL 09104+4109, using the best-fit FC95 King model  $r_{\text{core}}=30''$ ,  $kT=11.4\pm 3.2 \text{ keV}$ , and an extrapolated central surface brightness of 0.3–4.0 counts arcmin $^{-2} \text{ s}^{-1}$  (see Fig. 3 of FC95), we obtain from Eq. 3 a lower limit for  $n_{e,0}$  (electron density at the cluster center) in the range 0.027–0.097  $h_{50}^{1/2} \text{ cm}^{-3}$ . This is consistent with the value of  $\sim 0.038 h_{50}^{1/2} \text{ cm}^{-3}$  at  $r < 50 \text{ kpc}$  obtained from the deprojection analysis of Crawford & Vanderreist (1996), but we note once again that these values are upper limits for the true central densities, because of the cooling flows. Cooling flow gas should have roughly  $r^{-1}$  density and pressure profiles (Fabian 1994, p. 299), and the X-ray images do not resolve the innermost regions where the density should be highest. In addition, the apparent central X-ray deficit in IRAS 09104+4109 may alter conditions in the cluster center. For comparison, Abell clusters typically have  $n_{e,0}=0.001\text{--}0.010 h_{50}^{1/2} \text{ cm}^{-3}$  (Jones & Forman 1984), and the host clusters of the radio galaxies Cygnus A and 3C 295 have  $n_{e,0}=0.057\pm 0.016$  and  $> 0.026_{-0.009}^{+0.018} h_{50}^{1/2} \text{ cm}^{-3}$  respectively (Carilli, Perley & Harris 1994, HH86).

We can also constrain  $n_{e,0}$ ,  $t_{\text{cool}}$ , and  $\dot{M}_{\text{cool}}$  for the three RLQ host clusters. Using our upper limit surface brightnesses for  $r_{\text{core}}=125 \text{ kpc}$  and assuming  $kT=5 \text{ keV}$  ( $kT=2.5 \text{ keV}$  for 3C 206), we obtain the limits shown in Table 1. The limiting central surface brightnesses and density limits are lower and the cooling times longer for  $r_{\text{core}} > 125 \text{ kpc}$  and/or  $H_0 > 50$ , but can be shorter if the gas is abnormally cool or centrally concentrated (e.g. in galaxy size halos or clusters with  $r_{\text{core}} < 125 \text{ kpc}$ ). For 3C 206, the cooling time at the center of a putative cluster right at our  $3\sigma$  upper limit is less than the age of the universe at  $z=0.1976$  for plausible cosmologies. For 3C 263 and PKS 2352-342, if  $q_0=0.5$  the age of the universe at their redshifts is several Gyr shorter than the cooling times of their host clusters and thus no cooling flows are possible, but cooling flows are possible if  $q_0=0$ . If we assume  $q_0=0$  and make a maximal assumption of clusters just at our  $3\sigma$  upper limits with 50% of their emission from cooling flow components, we obtain the limits on  $\dot{M}_{\text{cool}}$  shown in Table 1. We discuss the implications of these values later, in §3.2.1.

Another interesting constraint on some of the clusters' line-of-sight properties can be made. H 1821+643 has significant flux below 912 Å (Kolman et al. 1991, Lee et al. 1993, Kriss et al. 1996); thus, the cooling flow in CL 1821+643 does not produce a Lyman limit and must have intrinsic  $N(\text{HI}) \leq 10^{17} \text{ cm}^{-2}$  along the line of sight. This is also the case for CL 3C 263 (Crawford et al. 1991) but not for CL 09104+4109, which has intrinsic  $N(\text{HI}) = 2.5_{-1.1}^{+1.8} 10^{21} \text{ cm}^{-2}$  (FC95). This latter value is typical for nearby cooling flows (Allen et al. 1995, but cf. Laor 1996); thus, the cooling flow in CL 1821+643 and any putative cooling flow in CL 3C 263 have unusually low intrinsic  $N(\text{HI})$  along our line of sight. Either the cooling flows have low overall  $N(\text{HI})$ , or, more likely, the ionizing radiation from the two quasars is confined to a cone (including our line of sight) within which cooling gas is reionized, as suggested by Bremer, Fabian & Crawford (1996).

### 3.2. Comparison of Observations and Models

In this section we compare our observations to three models which have been proposed to explain the evolution of AGN cluster environments. We introduce each model, discuss data on key predictions, point out problems, and discuss implications and possible solutions to the problems.

#### 3.2.1. The Cooling Flow Model

The cooling flow model (Fabian et al. 1986, Fabian & Crawford 1990) is not a model for quasar formation in cooling flows, but rather a model for how dense cooling flows can fuel AGN located within them in a self-sustaining manner. However, if it is to explain the evolution of RLQs and PRGs in clusters at  $z < 0.6$ , such objects must preferentially be found in cooling flow clusters for some reason, perhaps because radio galaxies in clusters have higher radio luminosity due to radio lobe confinement (Barthel & Arnaud 1996). This model is supported by the work of Bremer et al. (1992, and references therein), who find that extended line-emitting gas around  $z \lesssim 1$  RLQs is so common that it must be long-lived and therefore confined. If a hot ICM confines the gas, the required pressure is such that the ICM should have cooling flows of 100-1000  $M_{\odot}/\text{yr}$ . Fabian & Crawford (1990) outline a model where luminous quasars at  $z > 1$  are surrounded by dense cooling flows in subclusters. They show that an AGN of luminosity  $L$  in dense ( $P = nT \sim 10^8 \text{ K/cm}^3$ ) gas at the virial temperature of the central cluster galaxy ( $T \sim 10^7 \text{ K}$ ) will Compton-cool the gas within a radius  $R \propto L^{1/2}$  for a mass accretion rate (proportional to this volume) of  $\dot{M} \propto L^{3/2}$ . Since  $L \propto \dot{M}c^2$ , this Compton-cooled accretion flow will grow by positive feedback until  $L = L_{\text{Edd}}$ , as long as Compton cooling dominates brehmsstrahlung for  $L < L_{\text{Edd}}$ , which occurs only in high- $P$  environments. AGN so powered will last until a major subcluster merger or until the supply of dense cooling gas is exhausted. Assuming the most luminous objects form in the densest regions, the observed optical fading of the RLQ/PRG population in clusters below  $z \sim 0.6$  can be explained by major subcluster mergers (which occur earlier in the richest environments) disrupting the Compton-cooling mechanism, leading to a precipitous drop in the quasar luminosity. Thus this

model is also intriguingly consistent with the simulations of Tsai & Buote (1996) discussed in §1.

The cooling flow model can be tested in detail for 3C 263. Crawford et al. (1991), hereafter C91, predict  $\dot{M}_{\text{cool}}=100\text{--}1000 M_{\odot}/\text{yr}$  for CL 3C 263 from extended emission-line gas observations. We predict at most  $\dot{M}_{\text{cool}}<202 M_{\odot}/\text{yr}$  for CL 3C 263, and then only if  $q_0=0$ . For  $q_0=0.5$ , to have  $t_{\text{cool}}$  less than the age of the universe at its redshift and  $\dot{M}_{\text{cool}}=100 M_{\odot}/\text{yr}$ , CL 3C 263 must have either  $r_{\text{core}}<62$  kpc and cooling flow  $L_{X,44}=1.2$ , or  $T<1.3$  keV and cooling flow  $L_{X,44}=0.3$ , where  $L_{X,44}$  is X-ray luminosity in units of  $10^{44}$  erg  $\text{s}^{-1}$ . In addition, the minimum energy pressure 100 kpc from the quasar given by C91 can be produced by the ICM only if there is a cluster with  $kT=5$  keV and  $r_{\text{core}}=125$  kpc right at our upper limit luminosity. However, matching the pressure at  $<100$  kpc inferred by C91 from any of their models based on observed [OIII]/[OII] line ratios and various assumptions for the quasar’s ionizing spectrum requires an additional compact cooling flow component or a cluster with  $r_{\text{core}}\lesssim 100$  kpc. Thus for CL 3C 263 to match the predictions of the cooling flow model as given in C91, it cannot be much fainter than our upper limit and must have  $r_{\text{core}}\lesssim 60\text{--}100$  kpc and/or an unusually low  $kT$  for its  $L_X$ . Crawford & Fabian (1989) and Fabian (1992) point out, however, that since collapsed structures at high  $z$  have shallower potentials, the gas in them will have a lower  $kT$ , and since they are denser, “more compact objects than present-day clusters may be appropriate sites for remote cooling flows.”

The cooling flows in our two RQQ host clusters may very well have central ( $<1$  kpc) pressures  $\sim 10^8$  K/cm<sup>3</sup>, and thus be explained by the cooling flow model’s Compton feedback mechanism, again with the caveat for IRAS 09104+4109 that the apparent central X-ray deficit may indicate unusual conditions. But if pressures do reach  $10^8$  K/cm<sup>3</sup> at  $<1$  kpc in massive ( $\dot{M}\gtrsim 500 M_{\odot}/\text{yr}$ ) cooling flows at low redshift ( $z\lesssim 0.4$ ), this model must explain why surveys of powerful AGN at such redshifts very rarely find them in massive cooling flow clusters. Also, if our three RLQ host clusters have cooling flows at all, they would have  $\dot{M}\lesssim 200 M_{\odot}/\text{yr}$ . Central pressures  $\sim 10^7$  K/cm<sup>3</sup> have been estimated for cooling flows of this strength at low redshift (Heckman et al. 1989). Thus the central pressures in these RLQ host clusters are not likely to be consistent with the cooling flow model because their central pressures are an order of magnitude lower than required for the Compton-cooling feedback mechanism of Fabian & Crawford (1990) to successfully power the AGN. *This evidence suggests that the cooling flow model cannot be the sole explanation for the evolution of powerful AGN in clusters.* However, current data is insufficient to completely rule the model out as the sole explanation, since our three RLQ host clusters which seem to lack dense cooling flows *might* be powered in the manner predicted by this model *if* 1) cooling flows are in more compact and cooler clusters at high redshift or 2) there is something unusual about these objects which has caused the density of hot gas in their innermost regions to increase by at least an order of magnitude above the density predicted by X-ray data (cf. §3.3).

As for powerful FR II radio galaxies (PRGs), at low redshift they are extremely rarely found in clusters (which preferentially host FR I radio galaxies), and most of those that are in clusters are not at the cluster centers (Ledlow & Owen 1995, Wan & Daly 1996), which may in itself argue against the cooling flow model. The only two clusters with central FR II galaxies in which cooling

flows could have been definitively detected with observations of the S/N and spatial resolution made to date are CL 3C 295 and CL CygA, both of which have cooling flows of  $\sim 200 M_{\odot}/\text{yr}$  (see references in legend to Fig. 4). The next best candidate for a FR II radio galaxy at the center of a cooling flow is B3 1333+412 in A1763 at  $z=0.189$  (Vallée & Bridle 1982). For CL 3C 295, existing observations do not rule out high central pressures. For CL CygA, Reynolds & Fabian (1996) find  $P=2.5 \cdot 10^6 \text{ K/cm}^3$  at 15 kpc. This extrapolates to  $\sim 4 \cdot 10^7 \text{ K/cm}^3$  at  $r=1 \text{ kpc}$  assuming  $P \propto r^{-1}$  (Fabian 1994). So it is possible these two PRGs have central densities and pressures sufficient to support the Compton feedback quasar fueling mechanism, but it is also possible that some other process is needed to create the required high densities.

The finding of Wan & Daly (1996) that FR II host clusters at  $z \leq 0.6$  are typically X-ray underluminous (i.e. cooler or less dense than average clusters) may also be a problem for this model (cf. Fig. 4). The central densities they give clusters translate into cooling times longer than the age of the universe for all clusters in their sample except CL CygA. But Wellman, Daly & Wan (1996a, 1996b), using radio bridge parameters of a sample of FR II radio galaxies at  $z=0.5\text{--}1.8$ , derive somewhat larger surrounding densities and temperatures, consistent with present day ICM, and cooling times short enough to form cooling flows in some cases (cf. §3.2.2).

Thus the cooling flow model for the evolution of FR II AGN environments is unlikely to be the *sole* explanation for this evolution. H 1821+643 and IRAS 09104+4109 are easily explained by this model, but all other host clusters we have discussed may harbor cooling flows as dense as required by the model only if 1) cooling flows are found in cooler and denser clusters at  $z \gtrsim 0.4$ , or 2) some other mechanism has boosted their central densities high enough to engage the fueling mechanism proposed in the model. (However, Cygnus A and 3C 206 need not follow this model for it to explain the evolution of FR II AGN environments at  $z \gtrsim 0.4$ .) One possible mechanism for increasing central densities is strong interactions or mergers, discussed in §3.3.

### 3.2.2. The Low ICM Density Model

The low-ICM-density model (Stocke & Perrenod 1981, EYG91, Yee & Ellingson 1993) predicts that quasars are preferentially located in host clusters with low-density ICM ( $\lesssim 10^{-4} \text{ cm}^{-3}$ ) where ram pressure stripping is inefficient and gas remains in galaxies as a possible AGN fuel source. This model is consistent with findings that radio sources at  $z \sim 0.5$  have radio morphologies uncorrelated with the richnesses of their environs (Rector, Stocke & Ellingson 1995, Hutchings et al. 1996), implying that at  $z \sim 0.5$  the ICM/IGM in optically rich environments is not consistently denser than in poor ones. Similarly, Wan & Daly (1996) find that at  $z < 0.35$  clusters with FR II sources tend to be less X-ray luminous (less dense and/or cooler) than those without. FR II host clusters at  $z \sim 0.5$  are consistent with being underluminous as well, based on comparison of inferred radio bridge pressures to those in the  $z < 0.35$  sample. However, this model is inconsistent with Wellman, Daly & Wan (1996a, 1996b), who find from radio bridge studies that at  $z=0.5\text{--}1.8$  large FR II 3C radio galaxies may be surrounded by gas with densities and temperatures similar to nearby

clusters. These different results may be explained by the different radio powers of the objects in each sample (cf. Barthel & Arnaud 1996). Also, some high- $z$  radio galaxies are observed to have large rotation measures which at low  $z$  are caused only by dense ICM (Carilli et al. 1997).

This model predicts that powerful AGN host clusters are X-ray underluminous for their optical richnesses. In Figure 4 we plot cluster richness  $B_{gc}$  vs. rest-frame soft X-ray luminosity  $L_X(0.1-2.4 \text{ keV})$  to look for this trend.  $B_{gc}$  is a linear measure of richness. Quasar host clusters are plotted as filled squares, with upper limits assuming  $r_{core}=125 \text{ kpc}$ . Open squares are a  $\bar{z}\sim 0.3$  subsample of X-ray selected EMSS clusters studied by the CNOC group (Carlberg et al. 1996), radio galaxies are filled triangles, and other symbols are objects from the literature (see figure legend for references). The dotted line is the best-fit relation to the CNOC/EMSS data. Compared to both the CNOC sample and other clusters from the literature, H 1821+643 and IRAS 09104+4109 are X-ray overluminous for their optical richnesses and 3C 206, 3C 263, and PKS 2352–342 are either normal or underluminous, consistent with this model. Note, however, that several  $z>0.5$  optically selected clusters (half-filled squares; see figure legend for references) lie at the low- $L_X$  end of the literature range; thus, our two high- $z$  RLQ host clusters might be normal or even overluminous compared to high- $z$  optically selected clusters of similar richness.

Clusters with central FR II radio galaxies (filled triangles) are either normal or underluminous for their richnesses. The  $L_X$  for 3C 382 is probably contaminated by the central engine, as an archival WFPC2 image reveals a bright, unresolved source in the center of the host galaxy. Thus the only overluminous PRG host clusters are those of 3C 295 and Cygnus A, but these objects do present immediate problems for this model. Perley & Taylor (1991) argue convincingly that 3C 295 is  $<10 \text{ Myr}$  old, based on its observed size and the ram pressure needed to confine the hot spots. Similar calculations for Cygnus A yield an age of  $\sim 30-40 \text{ Myr}$  (Carilli et al. 1991, Blandford 1996). Multiple-generation AGN models predict characteristic lifetimes of  $\sim 100 \text{ Myr}$  and single-generation models even longer ones (Cavaliere & Padovani 1988), so these truly are young AGN. If the low-ICM-density model is correct and radio sources should not form in dense clusters, these clusters must have grown dense only after the radio sources formed. However, the shortest timescale on which the ICM might significantly evolve is the cluster-core sound crossing time,  $\sim 100 \text{ Myr}$ , so it appears some strong radio sources have formed while immersed in dense ICM.

The existence of these two high ICM density RQQ host clusters is a problem for the low ICM density model if it is to be a universal explanation for the presence and evolution of quasars in clusters. But as RQQs in clusters are rare, they may very well have different evolutionary histories than RLQs in clusters. One possibility is that the RQQs formed as RLQs when the clusters were less dense and have been continuously active ever since. Their evolution into RQQs sometime after formation might have been due to spin-down of the black hole (Bechtold et al. 1994) or the increasing density of their environments interfering with jet production (Rees et al. 1982).

In this scenario, even if we assume the ICM density doubles on a dynamical timescale, a rate ten times faster than simulations predict (Evrard 1990) but probably still consistent with data

on high- $z$  optically selected clusters (Castander et al. 1994), H 1821+643 and IRAS 09104+4109 must be quite old ( $\sim 10^9$  yr) to have formed in clusters with even moderately low ICM densities ( $n_{e,0} \lesssim 10^{-3} \text{ cm}^{-3}$ ). If these two RLQ host clusters are typical of  $z \sim 0.7$  RLQ host clusters, then with this assumed rapid evolution of the ICM density it is possible that these clusters could evolve to be as luminous as the two RQQ host clusters by  $z \sim 0.30\text{--}0.44$ , consistent with the suggestion that these RQQs were once RLQs. Another constraint comes from the mass of the central black hole in H 1821+643, which is estimated at  $M_{\text{BH}} = 3 \cdot 10^9 M_{\odot}$  (Kolman et al. 1993). If H 1821+643 has accreted continuously at the Eddington limit with a 10% efficiency for conversion of accreted matter into energy, it would have reached this  $M_{\text{BH}}$  after 0.9 Gyr, just consistent with the age necessary for formation in a low ICM density cluster. If the efficiency were any less, the black hole would have reached its estimated mass more quickly and the quasar would have to be younger. If the accretion rate were any less, the quasar would not likely be as luminous as it is.

Thus while these two RQQs could be very old continuously active quasars which formed as RLQs in moderately low ICM density clusters, the required rate of ICM density increase is extremely large, the different timescales involved agree for only a small range of parameters, and the requirement for continuous fueling of these rather luminous quasars at the Eddington rate for  $\sim 1$  Gyr is a difficult one to fulfill without invoking interactions which allow gas to flow into the center of the host galaxies. This scenario does make the testable prediction that if any remnant radio lobes exist around these objects, they should be very old.

The major drawback of this scenario is that it is not applicable to the two PRGs (Cygnus A and 3C 295), since those AGN are very young. One explanation which might be applicable to all four objects in high ICM density clusters is that they were created recently when their host galaxies underwent strong interactions. We defer discussion of this possibility to §3.3. In any case, *the existence of these four objects in high ICM density clusters is sufficient to rule out the low-ICM-density model as the sole explanation for the presence of powerful AGN in clusters*, even though current data do not rule out low density ICM being present in *most* powerful AGN host clusters.

### 3.2.3. The Low- $\sigma_v$ Interaction/Merger Model

The low- $\sigma_v$  interaction/merger model (Hutchings, Crampton & Campbell 1984, EYG91) predicts that quasars will be preferentially found in unvirialized, low velocity dispersion ( $\sigma_v$ ) clusters where the low- $\Delta v$  encounters needed for strong interactions and mergers are relatively common (Aarseth & Fall 1980). Ellingson, Green & Yee (1991) showed that the composite  $\sigma_v$  of quasar host clusters is lower than for comparably rich Abell clusters, consistent with this model.

To test this model, in Figure 5 we plot cluster richness  $B_{\text{gq}}$  vs. cluster velocity dispersion  $\sigma_v$ . Compared to the CNOC and literature data, 3C 206 has a slightly low  $\sigma_v$  for its richness while H 1821+643 is normal. The  $\sigma_v$  and  $B_{\text{gq}}$  of 3C 206 are representative of the ensemble quasar host

cluster of Ellingson, Green & Yee (1991). The host clusters of the PRGs Cygnus A and 3C 295 are outliers. Smail et al. (1997) give  $1670 \text{ km s}^{-1}$  (21 objects) for CL 3C 295, and  $\pm 250 \text{ km s}^{-1}$  uncertainty (Smail, personal communication). The redshift histogram of CL 3C 295 shows no evidence for subclustering or field contamination (Dressler & Gunn 1992). The  $\sigma_v$  of CL CygA, based on only five galaxies, is almost certainly an overestimate (Spinrad & Stauffer 1982).

Thus the few available measurements of quasar and FR II radio galaxy host cluster velocity dispersions are not particularly supportive of this model, although some measurements may suffer from field contamination (Smail et al. 1997). Of the two RQQs in our sample, no  $\sigma_v$  measurement exists for CL 09104+4109, and CL 1821+643 has a normal or high  $\sigma_v$  for its richness. Since the cluster  $\sigma_v$  evolves on the dynamical timescale during formation, we can make the same arguments about the age of H 1821+643 as we did in the previous discussion for the low-ICM-density model, namely that these RQQs could be old AGN which formed as RLQs when the cluster had a lower  $\sigma_v$ . But for CL 3C 295 and CL CygA, even if we assume  $\sigma_v \sim 850 \text{ km s}^{-1}$  for consistency with X-ray data (Henry & Henriksen 1986, Carilli et al. 1991) their velocity dispersions would still be normal or high for their richnesses, and these AGN are too young to have formed when their clusters had lower  $\sigma_v$ . As we discuss in the next section, however, there is another possible explanation for these exceptions to the low- $\sigma_v$  model which may preserve the model’s viability.

### 3.3. Which Model(s) Are Correct?

None of the three simple models purporting to explain the presence and evolution of powerful AGN in cluster centers seem able to explain all the observations at first glance. The low ICM density model cannot account for AGN in clusters with dense ICM (3C 295 & Cygnus A, and H 1821+643 & IRAS 09104+4109 unless they are very old; c.f. §3.2.2), but is consistent with our nondetection of ICM emission from RLQ host clusters. Some other recent radio and X-ray work supports this model (Rector, Stocke & Ellingson 1995, Hutchings et al. 1996, Wan & Daly 1996), but some does not (Wellman, Daly & Wan 1996a, 1996b; Crawford & Fabian 1996b). The cooling flow model requires very strong cooling flows, and thus has difficulty accounting for host clusters without luminous X-ray emission or with relatively weak cooling flows, but can explain the X-ray luminous host clusters of H 1821+643 and IRAS 09104+4109. And the low- $\sigma_v$  model has difficulty explaining 3C 295, H 1821+643, and Cygnus A, whose host clusters have apparently high  $\sigma_v$ ’s, although it is supported by the scarce data on RLQ host clusters (Ellingson, Yee & Green 1991).

The evidence suggests that neither the cooling flow nor the low-ICM-density models can be the sole explanation for the presence and evolution of powerful AGN in clusters. Strictly speaking, the low- $\sigma_v$  model cannot be the sole explanation either, since some powerful AGN reside in high- $\sigma_v$  clusters. However, even in high- $\sigma_v$  clusters, the low- $\Delta v$  interactions or mergers required by the low- $\sigma_v$  model can still occur, albeit rarely. *We suggest the possibility that AGN are produced in clusters solely by a strong interaction of their host galaxy with another galaxy in the cluster.* (We define a strong interaction as an interaction and/or merger which results in considerable gas flow

into the central regions of the post-interaction AGN host galaxy.) This would naturally favor host clusters with low  $\sigma_v$  (and possibly low ICM density), since strong interactions with gas-containing galaxies are more common in such clusters, but again, such interactions can occur in any cluster (Duc & Mirabel 1994) as well as in the field where most quasars exist. If this strong interaction scenario is correct, the distribution of AGN host cluster velocity dispersions should be biased to low values, but need not consist exclusively of low- $\sigma_v$  clusters. A large sample of AGN host cluster  $\sigma_v$ 's will be needed to test that prediction. A more easily testable prediction is that all host galaxies of quasars in clusters should show evidence of interaction with another galaxy.

It is also possible that strong interactions are not the sole formation process for AGN in clusters, and that the cooling flow model operates in some cases. Strong interactions may also allow the cooling flow model to operate in clusters it would not otherwise be able to, by providing a mechanism for increasing the ICM densities at the center of the host galaxies sufficiently high to switch on the Compton-feedback fueling mechanism. X-ray observations of additional powerful AGN in clusters will determine how prevalent the cooling flow model can be, and how necessary an additional mechanism for increasing the central densities is. Observations of the host galaxies of such quasars will determine how often mergers might provide that mechanism.

We now consider whether there is evidence for or against this strong interaction scenario in the far-IR and optical properties of the host galaxies of the AGN we have discussed (cf. Table 1).

**Far-IR Properties: RQQs:** Both IRAS 09104+4109 and H 1821+643 are luminous far-IR sources (Table 1), with a  $60\mu\text{m}$  to optical luminosity ratio at least 2.5 times greater than any of our three RLQs. This excess far-IR emission above what is expected for quasars of their luminosity can plausibly be attributed to an excess of gas and dust in the RQQ host galaxies resulting from a recent strong interaction. The excess IR luminosity is too strong to be attributed to gas and dust in the cooling flow (Bregman, McNamara & O'Connell 1990). **RLQs:** The far-IR luminosity of 3C 206 is almost two orders of magnitude lower than the two RQQs. Both 3C 263 and PKS 2352–342 cannot be ruled out as being IR-luminous, although at most they would still be an order of magnitude less luminous than the two RQQs. Thus any interactions in which these RLQs were involved must have been much less gas-rich than those in which the RQQs were involved. **PRGs:** 3C 295 has  $\log L_{60\mu\text{m}} < 12.06 L_{\odot}$  (Golombek, Miley & Neugebauer 1988), and Cygnus A has  $\log L_{60\mu\text{m}} = 11.72 L_{\odot}$ , luminosities roughly an order of magnitude lower than those of the two RQQs. The far-IR luminosity could still be produced by interaction-induced starbursts, but it could also be reprocessed AGN emission. Since it is impossible to disentangle the two, the far-IR luminosities for these two radio galaxies are inconclusive. We note that CO(1-0) observations have been made of Cygnus A (Barvainis & Antonucci 1994, Evans 1996) and CO(3-2) observations of IRAS 09104+4109 (Evans 1996). Neither object was detected, but it is unclear how to extrapolate these cold gas mass limits to total gas mass limits, particularly if the gas is very near the central engine (or if it is immersed in a dense, hot cooling flow), as Barvainis & Antonucci point out.



**Optical Properties: RQQs:** The host galaxy of H 1821+643 is a featureless red cD galaxy which is slightly asymmetrical and offset from the nucleus by 1-2" (Hutchings & Neff 1991b). Hutchings & Neff (1991a) subjectively classify the galaxy as undergoing a weak interaction of somewhat old age. The host galaxy of IRAS 09104+4109 is a cD galaxy possibly in the midst of cannibalizing several smaller galaxies (Soifer et al. 1996). Hutchings & Neff (1991a) subjectively classify it as undergoing only a somewhat weak interaction of moderate age. Thus the optical evidence for mergers or strong interactions in these two RQQ host galaxies is suggestive but not strong. **RLQs:** A 600 sec archival WFPC2 image of 3C 206 shows strong evidence for interaction of its elliptical host galaxy with several smaller galaxies. The host galaxy's isophotes are slightly asymmetrically extended to the WNW, and two knots of emission, possibly galaxies being swallowed, appear within the host galaxy 1.5" SE and 0.5" W of the quasar. Projection effects cannot be ruled out, but the chances of such close projections occurring are quite small. A third galaxy, 4.25" SSW of the quasar, shows a faint nucleus inside a distorted envelope of low surface brightness emission, consistent with being tidally disrupted by the quasar host. A 280 sec archival WFPC2 image of 3C 263 shows five faint knots of emission within 5" of the quasar and a very faint, possibly asymmetrical, underlying envelope of emission. Better data are needed to determine the galaxy's morphology, as the current data do not rule out e.g. a luminous spiral galaxy host (which would however be unprecedented for a RLQ). No information is available on the host galaxy of PKS 2352–342. **PRGs:** An archival WFPC2 image of 3C 295 shows that its host galaxy is definitely disturbed, with distorted, asymmetrical isophotes and a partial shell or plume of emission. Optical evidence for interaction in Cygnus A (Smith & Heckman 1989, Stockton, Ridgway & Lilly 1994, Jackson et al. 1996) is less obvious but still strong: a secondary IR peak 1" north of the nucleus, substantial dust in the inner regions of the galaxy, counter-rotating gas structures and evidence for star formation in the nuclear region, and twisted isophotes (which might not indicate interaction, however; cf. Smith and Heckman 1989). Thus the 3C 295 host galaxy has almost certainly undergone a merger or strong interaction which could have begun any time within the last  $\sim$ Gyr, and Cygnus A probably also has been disturbed (as suggested by Stockton, Ridgway & Lilly 1994), but by a less disruptive or less recent event.

Thus while the evidence is not conclusive except in the case of 3C 295, it is on the whole supportive of a scenario where these AGN host galaxies have undergone strong interactions or mergers. Specifically, *in no case where data is available is no evidence for interaction seen*. This lends support to our suggestion that strong interactions may be the sole mechanism needed to explain the presence and evolution of powerful AGN in clusters.

However, the observations do not rule out the validity of the cooling flow model for at least some objects. While the cooling flow model need not be applicable to the host clusters of the low- $z$  AGN Cygnus A, 3C 206, and H 1821+643 for it to explain the evolution of FR II AGN environments at  $z \gtrsim 0.4$ , it should apply to the others. In IRAS 09104+4109 and possibly 3C 295, the central ICM densities may reach the values required by the cooling flow model without need for an additional mechanism. But in any case, the  $z \gtrsim 0.4$  AGN host galaxies show evidence for

having undergone strong interaction(s) capable of boosting the central densities sufficiently high for the Compton-cooling feedback mechanism to occur. (Average densities within the central  $\sim 100$  pc of up to  $2900 \text{ cm}^{-3}$  have been inferred from CO observations of interacting or merging gas-rich galaxies (Scoville et al. 1991).) Also, cooling flows may be preferentially located in more compact and cooler clusters at  $z \gtrsim 0.4$ , which would make their detection more difficult in our data.

In summary, we suggest that strong interactions with gas-containing galaxies may be the only mechanism needed to explain the presence and evolution of powerful AGN in clusters. This suggestion is consistent with the far-IR and optical properties of the host galaxies of the AGN discussed in this paper, despite the rarity of such encounters in the high- $\sigma_v$ , high ICM density cluster environments of some of those AGN. However, the cooling flow model cannot be ruled out for at least some objects. The data most needed to help determine the relative importance of each process are X-ray imaging, optical imaging, and  $\sigma_v$  measurements of powerful AGN host clusters. The strong interaction scenario predicts that the host galaxies of all AGN in clusters should show signs of interaction, and that the host clusters will rarely have high velocity dispersions, and rarely high X-ray luminosities and ICM densities as well. The cooling flow model predicts that FR II AGN host clusters at high  $z$  should have cooling flows, but not necessarily at low  $z$ .

#### 4. Conclusions

We report a limit of  $1.63 \cdot 10^{44} \text{ ergs s}^{-1}$  on the rest-frame 0.1-2.4 keV X-ray luminosity of the host cluster of the RLQ 3C 206 (assuming  $r_{\text{core}}=125 \text{ kpc}$  and  $kT=2.5 \text{ keV}$ ) and a detection of  $L_X=3.74 \pm 0.57 \cdot 10^{44} \text{ ergs s}^{-1}$  for the host cluster of the RQQ H 1821+643 ( $H_o=50$ ,  $q_o=0.5$  for both values). CL 1821+643 is one of the most X-ray luminous clusters known, overluminous for its optical richness (also the case for IRAS 09104+4109), and it has a cooling flow of  $\dot{M}_{\text{cool}}=1120 \pm 440 \text{ h}_{50}^{-2} M_{\odot} \text{ yr}^{-1}$ . Its existence complicates interpretation of X-ray spectra of this field (Appendix A). In particular, the observed Fe  $K\alpha$  emission is probably solely due to the cluster, and either the quasar is relatively X-ray quiet for its optical luminosity or the cluster has a relatively low temperature for its luminosity.

We combine our data with the recent observation of X-ray emission from the host cluster of the buried RQQ IRAS 09104+4109 (Fabian & Crawford 1995), our previous upper limits for two RLQs at  $z \sim 0.7$  (Hall et al. 1995), and literature data on FR II radio galaxies. We compare this dataset to the predictions of three simple models for the presence and evolution of powerful AGN in clusters: the cooling flow model, the low-ICM-density model, and the low- $\sigma_v$  model.

In the cooling flow model (§3.2.1), FR II AGN host clusters at  $z \gtrsim 0.4$  have dense cooling flows. Cooling flows have been detected in a few PRG and RQQ host clusters (Cygnus A, H 1821+643, IRAS 09104+4109, 3C 295). However, three RLQ host clusters (PKS 2352–342, 3C 263, 3C 206) have  $\dot{M}_{\text{cool}} \lesssim 200 M_{\odot}/\text{yr}$ , unless cooling flows are preferentially found in cooler, denser clusters at high  $z$  or some mechanism besides the cooling flow has increased the central densities in those

clusters to create the high central pressures required by this model. Strong interactions with gas-containing galaxies could be that mechanism. Nevertheless, it is likely that the cooling flow model is not the *sole* explanation for the presence and evolution of powerful AGN in clusters.

In the low-ICM-density model (§3.2.2), FR II AGN form in low-density ICM clusters and are destroyed as the ICM density increases. The three RLQs in our sample have host clusters consistent with this model, but the two FR II PRGs and the two RQQs have high-density host clusters overluminous for their optical richnesses. This is consistent with recent radio and X-ray studies of radio sources in different environments at  $z \sim 0.5$  which show no evidence for dense ICM in the majority of powerful AGN host clusters at that redshift (Rector, Stocke & Ellingson 1995, Hutchings et al. 1996, Wan & Daly 1996), but not with radio work around  $z \sim 1$  PRGs which infers gas densities and temperatures similar to nearby clusters (Wellman, Daly & Wan 1996ab, Carilli et al. 1997), or X-ray work which detects extended emission with  $L_X \sim 10^{44}$  erg  $s^{-1}$  around  $z > 1$  radio galaxies (Smail & Dickinson 1995, Crawford & Fabian 1996a, 1996b). These data show that the low-ICM-density model cannot be the only mechanism behind the presence and evolution of powerful AGN in clusters. Nonetheless, it is possible that most powerful AGN host clusters have low ICM densities, and that the exceptions are either old AGN which originally formed when the cluster ICM was less dense, or rare cases of strong interactions with galaxies which retained some of their gas in high-ICM density environments.

In the low- $\sigma_v$  interaction/merger model (§3.2.3), FR II AGN are preferentially found in clusters with low velocity dispersions, where the strong interactions which can create powerful AGN are more common. Only a handful of  $\sigma_v$  measurements for powerful AGN host clusters exist. The measurements of CL 3C 206 and the composite quasar host cluster of EYG91 support this model, those of CL 3C 295 and CL 1821+643 do not, and CL CygA lacks an accurate  $\sigma_v$  determination. More data are needed to be definitive.

We suggest that strong interactions with gas-containing galaxies may be the only mechanism needed to explain the presence and evolution of powerful AGN in clusters. The far-IR and optical properties of the host galaxies of the AGN discussed in this paper are consistent with this strong interaction scenario (§3.3), despite the rarity of such encounters in the high- $\sigma_v$ , high ICM density cluster environments of some of those AGN. However, the cooling flow model cannot be ruled out for at least some objects. The relative importance of strong interactions and cooling flows can be determined by testing the predictions of the models with future observations. The cooling flow model predicts that FR II AGN at  $z \gtrsim 0.4$  will be found in dense cooling flow clusters and that if the cooling flows do not provide the necessary high central pressures for the Compton-cooling feedback mechanism to work, there should be evidence for an additional process which has increased the pressure, such as a strong interaction with a gas-containing galaxy. The strong interaction scenario predicts that the host galaxies of all AGN in clusters should show signs of interaction, and that the host clusters will rarely have high velocity dispersions or high X-ray luminosities and ICM densities. Unlike the cooling flow model, the strong interaction scenario has the advantage that it is applicable to FR II AGN in all environments, not just clusters.

To definitively rule out some of the models we have considered and to advance our understanding of the relationships between powerful AGN and their host clusters, the following data will be needed: 1) more X-ray observations of FR II AGN in clusters, especially those for which extended emission-line regions have been studied by Bremer et al. (1992) and others, to ascertain whether these AGN host clusters are more likely to have cooling flows or low-density ICM (*ROSAT* HRI data on 3C 215 and 3C 254 received after this paper was submitted do not show luminous cluster X-ray emission); 2) accurate measurements of  $\sigma_v$  (and  $B_{gq}$  where necessary) for FR II AGN host clusters, to test the low- $\sigma_v$  model; 3) more detailed studies and modelling of the host galaxy properties of AGN in clusters, to rigorously test our strong interaction scenario for their origins; 4) optical and X-ray studies of the rare RQQs in rich clusters, to determine the properties of their host clusters and why they are not radio-loud AGN; 5) searches for extended low-frequency emission from remnant radio lobes around H 1821+643 and IRAS 09104+4109, to test the idea that these RQQs were once RLQs.

We thank Julio Navarro and the referee for their helpful comments and the *ROSAT* AO6 TAC for their support of this project and for pointing out the existence of the archival *EINSTEIN* observation of 3C 206 to us. This research has made use of data obtained through the High Energy Astrophysics Science Archive Research Center Online Service, provided by the NASA-Goddard Space Flight Center; data from the NRAO VLA Sky Survey obtained through the Astronomy Digital Image Library, a service of the National Center for Supercomputing Applications; data from operations made with the NASA/ESA Hubble Space Telescope, obtained from the data archive at the Space Telescope Science Institute, which is operated by the Association of Universities for Research in Astronomy, Inc., under NASA contract NAS 5-26555; and data from the IRAS archive at the Infrared Processing and Analysis Center and the NASA/IPAC Extragalactic Database (NED), which are operated by the Jet Propulsion Laboratory, California Institute of Technology, under contract to NASA. PBH acknowledges support from an NSF Graduate Fellowship and from NASA funding for analysis of *ROSAT* observations.

### A. X-ray Properties of Objects in the Field of H 1821+643

The field of H 1821+643 has been extensively monitored in the optical (Ulrich et al. 1992, Kolman et al. 1993, hereafter K93), UV (Kolman et al. 1991, Ulrich et al. 1992, Lee et al. 1993, K93), EUV (Fruscione et al. 1995), and X-ray (Pravdo & Marshall 1984, Warwick, Barstow & Yaqoob 1989, Kii et al. 1991, Williams et al. 1992, Ulrich et al. 1992, Yaqoob et al. 1993, K93, Yaqoob & Serlemitsos 1994, Yamashita et al. 1994). Confirmation of the existence of a luminous cooling flow cluster surrounding the quasar complicates the interpretation of previous X-ray observations of the field, since even the *ROSAT* PSPC could not readily resolve the emission from CL 1821+643, although it did resolve the white dwarf K1-16 from H 1821+643.

To assist in future modelling, in Table 3 we present basic parameters for the different

components as measured with the *ROSAT* HRI. Column one gives the *total* HRI count rate for each component, calculated from the fits made to the radial profiles extracted from the HRI image. Converting from cts s<sup>-1</sup> to flux requires assuming an absorbing column density and spectrum for each component. We assume a Galactic log N<sub>H</sub>=20.58 (Lockman & Savage 1995). The *ROSAT* HRI has extremely limited energy resolution, so the spectral parameters of the different components cannot be computed from our data alone. However, K93 have fit the combined spectra of the cluster and quasar using *ROSAT* PSPC data, whose energy response is more similar to the HRI than any other instrument. We use their spectral parameters for the quasar and white dwarf, but neglect the observed soft excess component of the quasar spectrum. We obtain a total unabsorbed quasar plus cluster flux of 3.97 10<sup>-11</sup> ergs cm<sup>-2</sup> s<sup>-1</sup>, compared to the 5.63 10<sup>-11</sup> ergs cm<sup>-2</sup> s<sup>-1</sup> found by K93 (calculated from L<sub>X</sub> in their Table 1). The difference can be entirely explained by the soft excess; attributing 10% of our observed quasar flux to a blackbody soft excess (Saxton et al. 1993) with kT=0.04 keV would result in a flux equal to that of K93.

Although spectral fitting is really needed to do so, we can use previous X-ray observations of this field in conjunction with our spatially resolved emission measurements to obtain useful information about the cluster and quasar properties. In the following discussion all luminosities are in the quasar *rest frame* bandpasses and scale as h<sub>50</sub><sup>-2</sup>. All hard X-ray measurements since 1980 are consistent with L<sub>X</sub>(2-10 keV) = 8.2 10<sup>45</sup> erg s<sup>-1</sup> (Yaqoob et al. 1993). With a cluster L<sub>X</sub>(0.1-2.4 keV)=2.33±0.57 10<sup>45</sup> erg s<sup>-1</sup> ignoring the cooling flow component, we expect a cluster L<sub>X</sub>(2-10 keV)=5.62 10<sup>45</sup> erg s<sup>-1</sup> for a 10.5 keV thermal brehmsstrahlung (TB) spectrum. If the quasar has a 2-10 keV to B-band flux ratio equal to the lowest observed among the other eleven quasars in the sample of Williams et al. (1992), then 34% of the observed 2-10 keV emission would be from the quasar and 66% from the cluster, for a cluster L<sub>X</sub>(2-10 keV)=5.41 10<sup>45</sup> erg s<sup>-1</sup>, consistent with expectations for a 10.5 keV TB spectrum. Using a Raymond-Smith spectrum to calculate the bandpass correction should not change these results drastically. A possible problem with a single-temperature TB spectrum is that the 2-10 keV (and indeed the 2-18 keV) spectrum is consistent with a smooth power law, the only significant residual feature being a probable 6.6 keV Fe K $\alpha$  line redshifted to 5.1 keV (Kii et al. 1991, Yaqoob et al. 1993, Yaqoob & Serlemitsos 1994, Yamashita et al. 1994). If 66% of the 2-10 keV flux was from a 10.5 keV TB spectrum and 34% from a power law, we might expect a spectral break or residual feature near 8.1 keV (observed). A detailed fit is needed to determine how strong such a residual would be; its apparent absence might simply be due to insufficient S/N in existing spectra (Yaqoob 1996, personal communication), or might indicate a multiphase (non-isothermal) cluster whose integrated spectrum better resembles a power law. A range of temperatures is in fact expected for the cooling flow emission component (i.e. the emission from gas cooling from the dominant cluster temperature kT), which we have neglected so far. Roughly speaking, we expect k $\bar{T}$ <sub>CF</sub>=0.5kT (Johnstone et al. 1992), using a cooling function  $\Lambda(T)\propto T^{1/2}$  (Sarazin 1988). Energetically, for kT~7 keV and k $\bar{T}$ <sub>CF</sub>~3.5 keV, we can self-consistently ascribe 66% of the 2-10 keV emission

to the cluster and cooling flow component. This  $kT$  is slightly low but is still within the range expected for the cluster's  $L_X$  and  $\sigma_v$ . In either case, the Fe  $K\alpha$  line of  $EW \sim 140$  eV observed by ASCA (Yamashita et al. 1994) can probably be explained by cluster emission alone.

We qualitatively conclude that the 2-10 keV spectrum of this field can be consistent with  $kT = 10.5$  keV cluster emission, provided that the quasar is somewhat X-ray quiet. More likely, there is a range of temperatures in the cluster and the average temperature is  $< 10.5$  keV. This is particularly true if the quasar is more normal in its X-ray/optical properties, since attributing more 2-10 keV flux to the quasar translates directly into a lower average temperature for the cluster. To make these constraints truly quantitative requires refitting existing X-ray spectra while incorporating our spatially resolved emission constraints in the HRI band.

## REFERENCES

- Aarseth, S.J., and Fall, S.M. 1980, ApJ 236, 43
- Abramopoulos, F., and Ku, W. H.-M. 1983, ApJ 271, 446
- Allen, S.W. 1995, MNRAS 276, 947
- Allen, S.W., Edge, A.C., Fabian, A.C., Boehringer, H., Ebeling, H., Johnstone, R.M., Naylor, T., and Schwarz, R.A. 1992, MNRAS 259, 67
- Allen, S.W., Fabian, A.C., Edge, A.C., Boehringer, H., and White, D.A. 1995, MNRAS 275, 741
- Allington-Smith, J.R., Ellis, R.S., Zirbel, E.L., and Oemler, Jr., A.O. 1993, ApJ 404, 521
- Antonucci, R. 1993, ARA&A 31, 473
- Arnaud, K. A., Fabian, A.C., Eales, S.A., Jones, C., and Forman, W. 1984, MNRAS 211, 981
- Arnaud, K. A. 1988, in *Cooling Flows in Clusters and Galaxies*, ed. A.C. Fabian (Dordrecht: Kluwer)
- Bahcall, N. A. 1981, ApJ 247, 787
- Barthel, P. D., and Arnaud, K. 1996, MNRAS 283, L45
- Barthel, P. D., and Miley, G. K. 1988, Nature 333, 319
- Barvainis, R., and Antonucci, R. 1994, AJ 107, 1291
- Bechtold, J., Elvis, M., Fiore, F., Kuhn, O., Cutri, R.M, McDowell, J.C., Rieke, M., Siemiginowska, A., and Wilkes, B.J. 1994, AJ 108, 759
- Birkinshaw, M., and Worrall, D.M. 1993, ApJ 412, 568
- Blandford, R. 1996, in *Cygnus A – Study of a Radio Galaxy*, eds. C.L. Carilli and D.E. Harris (Cambridge: Cambridge)
- Blundell, K.M., and Lacy, M. 1995, MNRAS 274, L9
- Blundell, K.M., Beasley, A. J., Lacy, M., and Garrington, S.T. 1996, ApJ, in press (astro-ph/9606102)
- Boehringer, H., Voges, W., Fabian, A.C., Edge, A.C., and Newmann, D.M. 1993, MNRAS 264, L25
- Bower, R.G., Boehringer, H., Briel, U.G., Ellis, R.S., Castander, F.J., and Couch, W.J. 1994, MNRAS 268, 345

- Bregman, J.N., McNamara, B.R., and O’Connell, R.W. 1990, ApJ 351, 406
- Bremer, M.N., Fabian, A.C., Crawford, C.S., and Johnstone, R.M. 1992, MNRAS 254, 614
- Bremer, M.N., Fabian, A.C., and Crawford, C.S. 1996, in *Cold Gas at High Redshift*, eds. Bremer et al. (Dordrecht: Kluwer)
- Briel, U.G., and Henry, J.P. 1993, A&A 278, 379
- Burg, R., Giacconi, R., Forman, W., and Jones, C. 1994, ApJ 422, 37
- Burns, J.O. 1990, AJ 99, 14
- Canizares, C.R., Fabbiano, G., and Trinchieri, G. 1987, ApJ 312, 503
- Carilli, C.L., Perley, R.A., Dreher, J.W., and Leahy, J.P. 1991, ApJ 383, 554
- Carilli, C.L., Perley, R.A., and Harris, D.E. 1994, MNRAS 270, 173
- Carilli, C.L., Röttgering, H.J.A., van Ojik, R., Miley, G.K., and van Breugel, W.J.M. 1997, ApJS in press
- Carlberg, R.G., Yee, H.K.C., Ellingson, E., Abraham, R., Gravel, P., Morris, S., and Pritchet, C. 1996, ApJ 462, 32
- Castander, F.J., Ellis, R.S., Frenk, C.S., Dressler, A., and Gunn, J.E. 1994, ApJ 424, L79
- Cavaliere, A., and Padovani, P. 1988, ApJ 315, 411
- Cen, R., and Ostriker, J.P. 1994, ApJ 429, 4
- Condon, J.J., Cotton, W.D., Greisen, E.W., Yin, Q.F., Perley, R.A., and Broderick, J.J., 1994, preprint (<http://www.cv.nrao.edu/~jcondon/nvss.html>)
- Crawford, C.S., Fabian, A.C., George, I.M., and Naylor, T. 1991, MNRAS 248, 139
- Crawford, C.S., and Fabian, A.C. 1993, MNRAS 239, 219
- Crawford, C.S., and Fabian, A.C. 1993, MNRAS 260, L15
- Crawford, C.S., and Fabian, A.C. 1995, MNRAS 273, 827
- Crawford, C.S., and Fabian, A.C. 1996a, MNRAS 281, L5
- Crawford, C.S., and Fabian, A.C. 1996b, MNRAS 282, 1483
- Crawford, C.S., and Vanderreist, C. 1996, MNRAS 281, in press
- David, L.P., Harnden, F.R., Jr., Kearns, K.E., and Zombeck, M.V. 1995, The ROSAT High Resolution Imager (HRI) (US ROSAT Science Data Center/SAO) (D95)
- Donahue, M., and Stocke, J. T. 1995, ApJ 449, 554
- DeRobertis, M., and Yee, H. K. C. 1990, AJ 100, 84
- Dressler, A., and Gunn, J.E. 1994, ApJS 78, 1
- Duc, P.-A., and Mirabel, I.F. 1994, A&A 289, 83
- Ebeling, H., Voges, W., Boehringer, H., Edge, A.C., Huchra, J.P., and Briel, U.G. 1996, MNRAS, in press (astro-ph/9602080)
- Edge, A.C., and Stewart, G.C. 1991a, MNRAS 252, 414
- Edge, A.C., and Stewart, G.C. 1991b, MNRAS 252, 428
- Edge, A.C., Fabian, A.C., Allen, S.W., Crawford, C.S., White, D.A., Boehringer, H., and Voges, W. 1994a, MNRAS 270, L1

- Edge, A.C., Boehringer, H., Guzzo, L., Collins, C.A., Neumann, D., Chincarini, G., De Grandi, S., Duemmler, R., Ebeling, H., Schindler, S., Weitter, W., Vettolani, P., Briel, U., Cruddace, R., Gruber, R., Gursky, H., Hartner, G., MacGillivray, H.T., Schuecker, P., Shaver, P., Voges, W., Wallin, J., Wolter, A., and Zamorani, G. 1994b, *A&A* 289, L34
- Elbaz, D., Arnaud, M., and Boehringer, H. 1995, *å* 293, 337
- Ellingson, E., Yee, H. K. C., Green, R. F., and Kinman, T.D. 1989, *AJ* 97, 6
- Ellingson, E., Green, R. F., and Yee, H. K. C. 1991, *ApJ* 378, 476
- Ellingson, E., Yee, H. K. C., and Green, R. F. 1991, *ApJ* 371, 36 (EYG91)
- Ellingson, E., and Yee, H. K. C. 1994, *ApJS* 92, 33
- Elvis, M., Lockman, F.J., and Wilkes, B.J. 1989, *AJ* 97, 777
- Evans, A.S. 1996, PhD Thesis, University of Hawaii.
- Evrard, A.E. 1990, *ApJ* 363, 349
- Fabian, A. C., and Crawford, C. S. 1990, *MNRAS* 247, 439
- Fabian, A. C., and Crawford, C. S. 1995, *MNRAS* 274, L63
- Fabian, A. C., Arnaud, K. A., Nulsen, P. E. J., and Mushotzky, R. F. 1986, *ApJ* 305, 9
- Fabian, A. C., in *Clusters and Superclusters of Galaxies*, ed. A.C. Fabian (Dordrecht: Kluwer), 151
- Fabian, A. C., *ARA&A* 32, 277
- Fabian, A. C., Shioya, Y., Iwasawa, K., Nandra, K., Crawford, C., Johnstone, R., Kuneida, H., McMahon, R., Makishima, K., Murayama, T., Ohashi, T., Tanaka, Y., Taniguchi, Y., and Terashima, Y. 1994, *ApJ* 436, L54
- Fabbiano, G., Miller, L., Trinchieri, G., Longair, M., and Elvis, M. 1984, *ApJ* 277, 115
- Fabricant, D.G., McClintock, J.E., and Bautz, M.W. 1991, *ApJ* 381, 33
- Fabricant, D.G., Bautz, M.W., and McClintock, J.E. 1994, *AJ* 107, 8
- Fruscione, A., Drake, J.J., McDonald, K., and Malina, R.F. 1995, *ApJ* 441, 726
- Gioia, I.M., and Luppino, G.A. 1994, *ApJS* 94, 583
- Golombek, D., Miley, G.K., and Neugebauer, G. 1988, *AJ* 95, 26
- Hall, P. B., Ellingson, E., Green, R. F., and Yee, H. K. C. 1995, *AJ*, 110, 513.
- Harris, D. E., ed., 1984, *The EINSTEIN Observatory Revised Users Manual* (Cambridge, Harvard/CfA)
- Heckman, T.M., Baum, S.A., van Breugel, W.J.M., & McCarthy, P. 1989, *ApJ* 338, 48
- Henry, J.P., Gioia, I.M., Maccacaro, T., Morris, S.L., Stocke, J.T., and Wolter, A. 1992, *ApJ* 386, 408
- Henry, J.P., and Henriksen, M. J. 1986, *ApJ* 301, 689 (HH86)
- Hill, G. J., and Lilly, S. J. 1991, *ApJ* 367, 1
- Hines, D. C., and Wills, B. J. 1993, *ApJ* 415, 82
- Hughes, J.P., Birkinshaw, M., and Huchra, J.P. 1995, *ApJ* 448, L93
- Hutchings, J. B., Crampton, D., and Campbell, B. 1984, *ApJ* 280, 41



- Hutchings, J. B. 1987, ApJ 320, 122
- Hutchings, J. B., and Neff, S. G. 1991, AJ 101, 434
- Hutchings, J. B., and Neff, S. G. 1991, AJ 101, 2001
- Hutchings, J. B., Gower, A. C., Ryneveld, S., and Dewey, A. 1996, AJ 111, 2167
- Jackson, N., Tadhunter, C., Sparks, W.B., Miley, G.K., and Macchetto, F. 1996, A&A 307, L29
- Johnstone, R.M., Fabian, A.C., Edge, A.C., and Thomas, P.A. 1992, MNRAS 255, 431
- Jones, C., and Forman, W., 1984, ApJ 276, 38
- Kii, T., Williams, O.R., Ohashi, T., Awaki, H., Hayashida, K., Inoue, H., Kondo, H., Koyama, K., Makino, F., Makishima, K., Saxton, R.D., Stewart, G.C., Takano, S., Tanaka, Y., and Turner, M.J.L. 1991, ApJ 367, 455
- Kleinmann, S.G., Hamilton, D., Keel, W.C., Wynn-Williams, C.G., Eales, S.A., Becklin, E.E., and Kuntz, K.D. 1988, ApJ 328, 161
- Kolman, M., Halpern, J.P., Shrader, C.R., and Filippenko, A.V. 1993, ApJ 373, 57
- Kolman, M., Halpern, J.P., Shrader, C.R., Filippenko, A.V., Fink, H.H., and Schaeidt, S.G. 1993, ApJ 402, 514
- Kriss, G., Krolik, J., Grimes, J., Tsvetanov, Z., Espey, B., Zheng, W., and Davidsen, A. 1996, in *Emission Lines in Active Galaxies: New Methods and Techniques*, eds. B.M. Peterson, F.-Z. Cheng, and A.S. Wilson (ASP: San Francisco) (astro-ph/9607154)
- Lacy, M., Rawlings, S., and Hill, G. J. 1992, MNRAS 258, 828
- Leahy, J.P., Muxlow, T.W.B., and Stephens, P.W. 1989, MNRAS 239, 401
- Le Brun, V., Bergeron, J., and Boissé, P. 1995, *â* 306, 691
- Ledlow, M. J., and Owen, F. N. 1995, AJ 109, 853
- Lee, G., Kriss, G.A., Zheng, W., and Davidsen, A.F. 1993, BAAS 182, 792
- Lockman, F.J., and Savage, B.D. 1995, ApJS 97, 1 (LS95)
- Longair, M.S. and Seldner, M. 1979, MNRAS 189, 433
- Luppino, G.A., and Gioia, I.M. 1995, ApJ 445, L77
- Mathieu, R.D., and Spinrad, H. 1981, ApJ 251, 485
- McNamara, B.R., Jannunzi, B.T., Elston, R., Sarazin, C., and Wise, M. 1996, ApJ, in press
- Miley, G.K., and Hartsuijker, A.P. 1978, A&AS 34, 129
- Morse, J. A. 1994, PASP 106, 675
- Navarro, J.F., Frenk, C.S., and White, S.D.M. 1996, ApJ 462, 563
- Nesci, R., Perola, G.C., and Wolter, A. 1994, A&AS 299, 34
- Neugebauer, G., Soifer, B. T., Miley, G. K.; Clegg, P. E 1986, ApJ 308, L1
- Nichol, R.C., Ulmer, M.P., Kron, R.G., Wirth, G.D., Koo, D.C. 1994, ApJ 432, 464
- Nulsen, P.E.J., Stewart, G.C., and Fabian, A.C. 1984, MNRAS 208, 185
- O’Dea, C.P., Worrall, D.M., Baum, S.A., and Stanghellini, C. 1996, AJ 111, 92

- Padovani, P., & Urry, C.M. 1991, ApJ 368, 373
- Papadopoulos, P. P., Seaquist, E.R., Wrobel, J.M., and Binette, L. 1995, ApJ 446, 150
- Perley, R.A., and Taylor, G.B. 1991, AJ 101, 1623
- Pierre, M., Boehringer, H., Ebeling, H., Voges, W., Schuecker, P., Cruddace, R., and MacGillivray, H. 1994, *Å* 290, 725
- Pierre, M., Hunstead, R., and Unewisee, A. 1994, in *Cosmological Aspects of X-Ray Clusters of Galaxies*, ed. W.C. Seiter, (Dordrecht:Kluwer), p. 73
- Pravdo, S.H., and Marshall, F.E. 1984, ApJ 281, 570
- Prestage, R.M., and Peacock, J.A. 1988, MNRAS 230, 131
- Quintero, Z.M., and Cersosimo, J.C. 1993, A&AS 97, 435
- Rawlings, S. 1994, in *The Physics of Active Galactic Nuclei*, eds. G.V. Bicknell, M.A. Dopita, and P.J. Quinn (San Francisco: ASP), 253
- Raymond, J.C., and Smith, B.W. 1977, ApJS 35, 419
- Rector, T.A., Stocke, J.T., and Ellingson, E. 1995, AJ 110, 1492
- Rees, M.J., Begelman, M.C., Blandford, R.D., and Phinney, E.S. 1982, Nature 295, 17
- Reynolds, C.S., and Fabian, A.C. 1996, MNRAS 278, 479
- Richstone, D., Loeb, A., and Turner, E.L. 1992, ApJ393, 477
- Roche, N., Shanks, T., Almaini, O., Boyle, B.J., Georgantopoulos, I., Stewart, G.C., and Griffiths, R.E. 1995, MNRAS 276, 706
- Sarazin, C. L. 1988, *X-Ray Emission from Clusters of Galaxies*, (Cambridge: Cambridge)
- Saxton, R.D., Turner, M.J.L., Williams, O.R., Stewart, G.C., Ohashi, T., and Kii, T. 1993, MNRAS 262, 63
- Schindler, S., Hattori, M., Neumann, D.M., and Boehringer, H. 1996, A&AS, submitted (astro-ph/9603037)
- Schmidt, M., and Green, R.F. 1986, ApJ 305, 68
- Schneider, D.P., Bahcall, J.N., Gunn, J.E., and Dressler, A. 1992, AJ 103, 1047
- Schwartz, D.A., Bradt, H.V., Remillard, R.A., and Tuohy, I.R. 1991, ApJ 376, 424
- Scoville, N.Z., Sargent, A.I., Sanders, D.B., and Soifer, B.T. 1991, ApJ 366, L5
- Smail, I., and Dickinson, M. 1995, ApJ 455, 99
- Smail, I., Couch, W.J., Ellis, R.S., and Sharples, R.M. 1995, ApJ 440, 501
- Smail, I., Ellis, R.S., Dressler, A., Couch, W.J., Oemler, Jr., A., Sharples, R.M., and Butcher, H. 1995, ApJ, in press
- Smith, E.P., and Heckman, T.M. 1989, ApJS 64, 365
- Soifer, B.T., Neugebauer, G., Armus, L., and Shupe, D.L. 1996, AJ 111, 649
- Soker, N., and Sarazin, C.L. 1988, ApJ 327, 66
- Spinrad, H., and Stauffer, J.R. 1982, MNRAS 200, 153
- Stocke, J. T. and Perrenod, S. C. 1981, ApJ 245, 375

- Stocke, J. T., Morris, S. L., Weymann, R. J. and Foltz, C. B. 1992, ApJ 396, 487
- Stockton, A., Ridgway, S.E., and Lilly, S.J. 1994, AJ 108, 414
- Struble, M.F., and Rood, H.J. 1987, ApJS 63, 543
- Teague, P.F., Carter, D., and Gray, P.M. 1990, AJ 72, 715
- Tsai, J.C., and Buote, D.A. 1996, MNRAS in press (astro-ph/9510057)
- Turner, M.J.L., and Pounds, K.A. 1989, MNRAS 240, 833
- Ulrich, M.-H., Fink, H.H., Schaeidt, S., Baganoff, F., Malkan, M.A., Heidt, J., and Wagner, S. 1992, *Å* 266, 183
- Vallée, J.P., and Bridle, A.H. 1982, ApJ 253, 479
- Wan, L., and Daly, R.A. 1996, ApJ, 467, 145
- Warwick, R.S., Barstow, M.A., and Yaqoob, T. 1989, MNRAS 238, 917
- Wellman, G.F., Daly, R.A., and Wan, L. 1996a, ApJ, in press
- Wellman, G.F., Daly, R.A., and Wan, L. 1996b, ApJ, in press
- White, D.A., Fabian, A.C., Allen, S.W., Edge, A.C., Crawford, C.S., Johnstone, R.M., Stewart, G.C., and Voges, W. 1994, MNRAS 269, 589
- Wilkes, B.J., Tananbaum, H., Worrall, D.M., Avni, Y., Oey, M.S., and Flanagan, J. 1994, ApJS 92, 53
- Williams, O.R., Turner, M.J.L., Steward, G.C., Saxton, R.D., Ohashi, T., Makishima, K., Kii, T., Inoue, H., Makino, F., Hayashida, K., and Koyama, K. 1992, ApJ 389, 157
- Worrall, D.M., Birkinshaw, M., and Cameron, R.A. 1995, ApJ 449, 93
- Yamashita, A., Kii, Tsuneko, Tashiro, M., Makishima, K., and Ohashi, T. 1994, in *New Horizon of X-ray Astronomy: First Results from ASCA*, eds. F. Makino and T. Ohashi, (Universal Academy Press:Tokyo), 599
- Yaqoob, T., Serlemitsos, P.J., Mushotsky, R.F., Weaver, K.A., Marshall, F.E., and Petre, R. 1993, ApJ 418, 638
- Yaqoob, T., and Serlemitsos, P.J. 1994, in *New Horizon of X-ray Astronomy: First Results from ASCA*, eds. F. Makino and T. Ohashi, (Universal Academy Press:Tokyo), 337
- Yates, M.G., Miller, L., and Peacock, J.A. 1989, MNRAS, 240, 129
- Yee, H. K. C., and Ellingson, E. 1993, ApJ 411, 43
- Yee, H. K. C. and Green, R. F. 1987, ApJ 319, 28
- Zabludoff, A.I., Huchra, J.P., and Geller, M.J. 1990, ApJS 74, 1
- Zhao, J.-H., Sumi, D.M., Burns, J.O., and Duric, N. 1993, ApJ 416, 51
- Zombeck, M.V., Conroy, M., Harnden, F.R., Roy, A., Braeuninger, H., Burkert, W., Hasinger, G., and Predehl, P. 1990, in Proc. SPIE Conference on EUV, X-Ray, and Gamma-Ray Instrumentation for Astronomy, ed. O.H.W. Siegmund and H.S. Hudson, Proc. SPIE 1344, p. 267

Table 1. Summary of Target Observations and Properties

	3C 206	3C 263	PKS 2352-342	H 1821+643	IRAS 09104+4109
RA (1950.)	08:37:27.95	11:37:09.34	23:52:50.62	18:21:41.89	09:10:32.84
Dec (1950.)	-12:03:54.2	+66:04:26.9	-34:14:39.5	+64:19:01.05	+41:08:53.61
$N_H$ , $10^{20}$ cm $^{-2}$	5.62	0.91	1.07	3.80	1.60
Observation Dates	11/16-19/1979	11/4-7/1991	5/18-6/13/1993	3/22/1994	11/8/94
Livetime, sec	62732.75	26036.41	40173.94	30591.15	7937
Redshift	0.1976	0.646	0.706	0.297	0.442
$D_{Luminosity}$ , $10^{27}$ cm	3.82	13.4	14.8	5.81	8.93
Quasar Properties					
$M_B$	-25.0	-26.6	-26.7	-27.2	-26.3 $\pm$ 0.9 <sup>a</sup>
$\log(L_{60\mu m}/L_\odot)$	11.18	<12.28	(12.4) <sup>b</sup>	13.0	13.2
$\log P_{20cm}$ , W Hz $^{-1}$	26.45	27.30	27.21	25.13	25.16
Radio Morphology	FR II	FR II	...	core+lobe?	FR I/II
LLS $^c$ kpc	799	342	(200) <sup>d</sup>	20	175
$M_{host}$ galaxy	-22.6 (r)	>-23.2 (B)	...	-24.1 (R)	-24.45 <sup>e</sup> (R)
Cluster Properties					
$B_{gq}$ , Mpc $^{-1.77}$	683 $\pm$ 197	993 $\pm$ 550	681 $\pm$ 280	1200 $\pm$ 200	1210 $\pm$ 293
$\sigma_v$ , km s $^{-1}$	500 $\pm$ 110	...	...	1046 $\pm$ 108	...
$r_{core}$ , kpc	(125)	(125)	(125)	176.8 $\pm$ 9.9	200
$L_{X,44}$ <sup>f</sup>	<1.63	<3.48	<3.09	37.4 $\pm$ 5.7	30.3 $\pm$ 2.6
$n_{e,0}$ <sup>g</sup> $10^{-3}$ cm $^{-3}$	<6.76 (7.01)	<7.34 (10.0)	<6.79 (9.56)	>81 $\pm$ 22	>(27-97)
$T_{cool}$ <sup>g</sup> Gyr	>6.8 (6.5)	>8.8 (6.5)	>9.5 (6.8)	<6.37 $\pm$ 1.24	<(3.65-1.01)
$L_{X,44}$ ; cooling flow <sup>g</sup>	<0.82 (0.90)	0 (<2.42)	0 (<2.21)	14.1 $\pm$ 4.7	9.09 $\pm$ 0.78
$\dot{M}_{cool}$ <sup>g</sup> $M_\odot$ yr $^{-1}$	<137 (150)	0 (<202)	0 (<184)	1120 $\pm$ 440	1003 $^{+202}_{-272}$
$P_{central}$ <sup>g</sup> $10^6$ cm $^{-3}$ K	<0.20 (0.20)	<0.43 (0.58)	<0.40 (0.55)	>9.9 $\pm$ 3.4	>(3.6-12.8)

Table 1—Continued

3C 206	3C 263	PKS 2352-342	H 1821+643	IRAS 09104+4109
--------	--------	--------------	------------	-----------------

Note. —  $H_0=50$  and  $q_0=\frac{1}{2}$  assumed, although values of  $n_e$ ,  $T_{\text{cool}}$ ,  $L_{X,44}$ , cooling flow, and  $\dot{M}_{\text{cool}}$  are also given in parentheses for  $H_0=50$  and  $q_0=0$ . Luminosities scale as  $h_{50}^{-2}$ , sizes as  $h_{50}^{-1}$ ,  $n_e$  as  $h_{50}^{1/2}$ , and  $T_{\text{cool}}$  as  $h_{50}^{1/2}$ .

<sup>a</sup>Unobscured estimate from Hines & Wills (1993), converted to  $H_0=50$ ,  $q_0=0.5$ .

<sup>b</sup>2.4-2.9 $\sigma$  IRAS SCANPI detection. Can be considered a 3 $\sigma$  upper limit.

<sup>c</sup>Largest linear size of the radio source, measured at 20 cm except for 3C 206 (6 cm).

<sup>d</sup>Very uncertain estimate. The NVSS (cf. Condon et al. 1994) shows PKS 2352-342 to be slightly resolved (52''6 vs. 46'' for a source 6' away). Modeling it as a gaussian yields the FWHM=200 kpc given here.

<sup>e</sup>Contaminated by strong narrow line emission.

<sup>f</sup>Rest-frame 0.1-2.4 keV luminosity in units of  $10^{44}$  erg s<sup>-1</sup>.

<sup>g</sup>Values for  $q_0=0$  are in parentheses after values for  $q_0=0.5$ , both assuming  $H_0=50$ . Total estimated central density includes cooling flow component; central densities for the King component only are  $14.7\pm 2.4$  and  $6.9\pm 1.4 \times 10^{-3}$  cm<sup>-3</sup> for H 1821+643 and IRAS 09104+4109 respectively. Central pressures calculated assuming  $kT=2.5$  keV for 3C 206,  $kT=5$  keV for 3C 263 and PKS 2352-342,  $kT=10.5\pm 2.2$  for H 1821+643, and  $kT=11.4$  for IRAS 09104+4109.

References. —  $N_H$ : Lockman & Savage (1995) for all except 3C 206: Elvis, Lockman & Wilkes (1989) and IRAS 09104+4109: Fabian et al. (1994).  $L_{60\mu\text{m}}$ : 3C 206 and 3C 263: Neugebauer et al. (1986); PKS 2352-342: this work; RQQs: Hutchings & Neff (1991a). Radio: 3C 206: Miley & Hartsuijker (1978); 3C 263: Hutchings et al. (1996); PKS 2352-342: Quinto & Cersosimo (1993) and Condon et al. (1994); H 1821+643: Kolman et al. (1993) and Blundell & Lacy (1995); IRAS 09104+4109: Hines & Wills (1993).  $M_{\text{host galaxy}}$ : 3C 206: Ellingson et al. (1989); 3C 263: Crawford et al. (1991); H 1821+643: Hutchings & Neff (1991b); IRAS 09104+4109: Kleinmann et al. (1988).  $B_{\text{gg}}$ : 3C 206: Ellingson et al. (1989); 3C 263, PKS 2352-342: Yee & Ellingson (1993); H 1821+643: Lacy, Rawlings & Hill (1992); IRAS 09104+4109: this work.  $\sigma_v$ : 3C 206: Ellingson et al. (1989); H 1821+643: this work. Cluster X-ray properties: this work or Paper I, except  $r_{\text{core}}$  and  $L_{X,44}$  (0.1-2.4 keV, observed) for IRAS 09104+4109, from Fabian & Crawford (1995).

Table 2. Quasar Host Cluster X-Ray Luminosities — Upper Limits and Detections

Core Radius H <sub>o</sub> , q <sub>o</sub>	125 kpc 50, 0.5	125 kpc 75, 0.5	125 kpc 50, 0.0	125 kpc 75, 0.0	250 kpc 50, 0.5	250 kpc 75, 0.5	250 kpc 50, 0.0	250 kpc 75, 0.0
3C 206	1.63	0.92	1.80	1.02	2.60	1.57	2.88	1.74
3C 263 <sup>a</sup>	3.48	1.86	4.83	2.58	5.10	3.26	7.08	4.52
PKS 2352-342 <sup>a</sup>	3.09	1.66	4.41	2.37	4.44	2.75	6.32	3.92
H 1821+643 <sup>b</sup>	51.5±10.	22.9±4.4	44.8±8.8	19.9±3.9	...	...	...	...
IRAS 09104+4109 <sup>c</sup>	...	...	...	...	30.3±2.6	13.5±1.2	38.0±3.2	16.9±1.4

Note. — Luminosities are in units of  $10^{44}$  ergs  $s^{-1}$  in the *rest-frame* 0.1–2.4 keV passband. Values with uncertainties are detections; all other values are  $3\sigma$  upper limits.

<sup>a</sup>These values are slightly larger than those of Table 2 in Paper I because they have been corrected to the rest-frame 0.1–2.4 keV passband.

<sup>b</sup>We find a best-fit  $r_{\text{core}}=176.8\pm 9.9 h_{50}^{-1}$  kpc ( $190.5\pm 9.6 h_{50}^{-1}$  kpc) for  $q_o=0.5$  (0).

<sup>c</sup>Fabian & Crawford (1995) find  $r_{\text{core}}=30''$ , or 200 (225) kpc for  $q_o=0.5$  (0), and a large cooling flow excess.

Table 3. Properties of Objects in the Field of H 1821+643

Component	HRI counts/s	Central S.B. <sup>a</sup>	$r_{\text{core}}/\sigma_{\text{gauss}}$	Spectrum <sup>b</sup>	ECF <sup>c</sup>	Unabsorbed Flux <sup>d</sup>
Quasar	0.3136±0.0032	...	...	PL, $\alpha=1.81$	0.100	3.136±0.032
Cluster <sup>e</sup>	0.1152±0.0163	1.77±0.15	32''2±1''8	RS, kT=5 keV	0.223	0.516±0.073
Cooling Flow <sup>f</sup>	0.0699±0.0233	36.03±11.63	5''56±0''46	RS, kT=5 keV	0.223	0.314±0.105
...	...	43.85±18.21	5''04±0''51	...	...	...
White Dwarf	0.0184±0.0011	...	...	BB, kT=0.01	0.00195	9.44±0.57

<sup>a</sup>Central surface brightness in units of  $10^{-5}$  ROSAT HRI counts  $s^{-1}$  arcsec $^{-2}$ .

<sup>b</sup>Spectrum assumed to convert counts to flux: PL=Power Law, RS=Raymond-Smith plasma, BB=blackbody.

<sup>c</sup>Energy to Counts conversion Factor, estimated from David et al. (1995).

<sup>d</sup>Observed 0.1-2.4 keV (rest-frame 0.13-3.11 keV) flux in units of  $10^{-11}$  ergs  $s^{-1}$  cm $^{-2}$ , corrected for Galactic absorption of  $\log N_{\text{H}}=20.58$  only.

<sup>e</sup>King model component only. The central surface brightness has been corrected by +1.9% and  $r_{\text{core}}$  by +3.6% to account for systematic errors in the fitting as measured from simulated data.

<sup>f</sup>Upper row values are not corrected for convolution with ROSAT HRI PRF; lower row values are corrected.

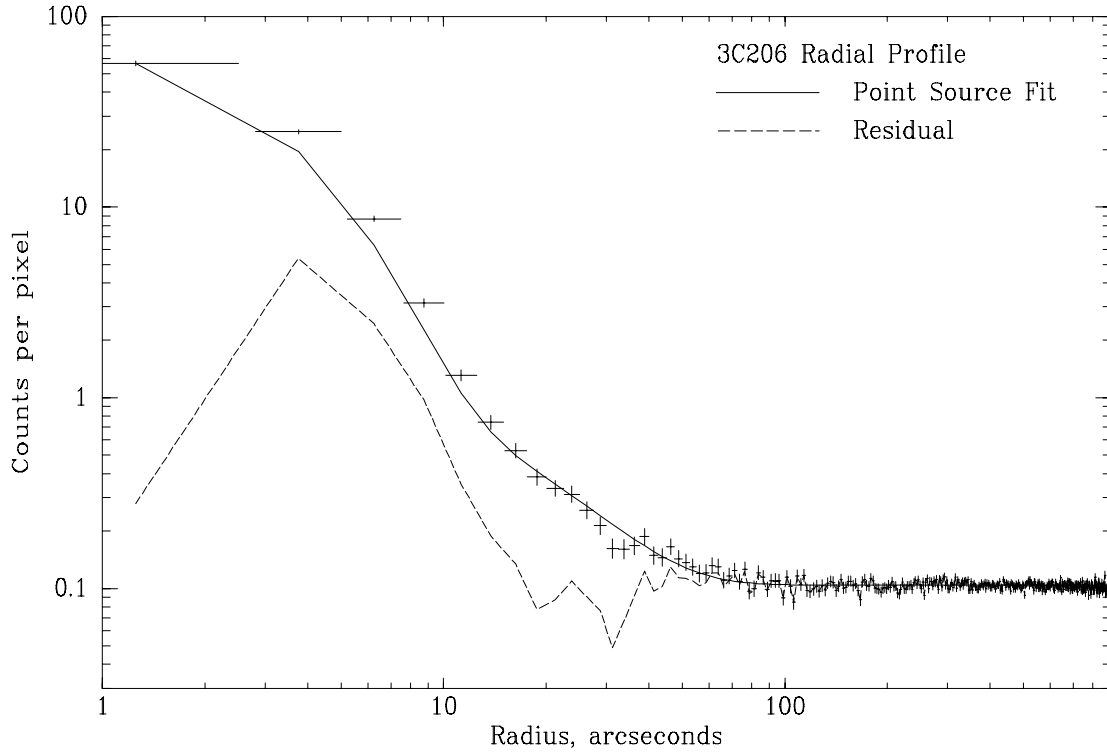


Fig. 1.— Radial profiles of the *EINSTEIN* HRI image of the quasar 3C 206, the fitted PRF and background, and the residual after subtraction of an *EINSTEIN* HRI point response function (PRF) normalized such that the residual is zero in the innermost bin. The residual is exaggerated in this log-log plot; note that the apparent excess emission is of the same scale as the PRF and that the background-subtracted residual is actually negative between 15-40'', exactly the region in which cluster emission should be most prominent.

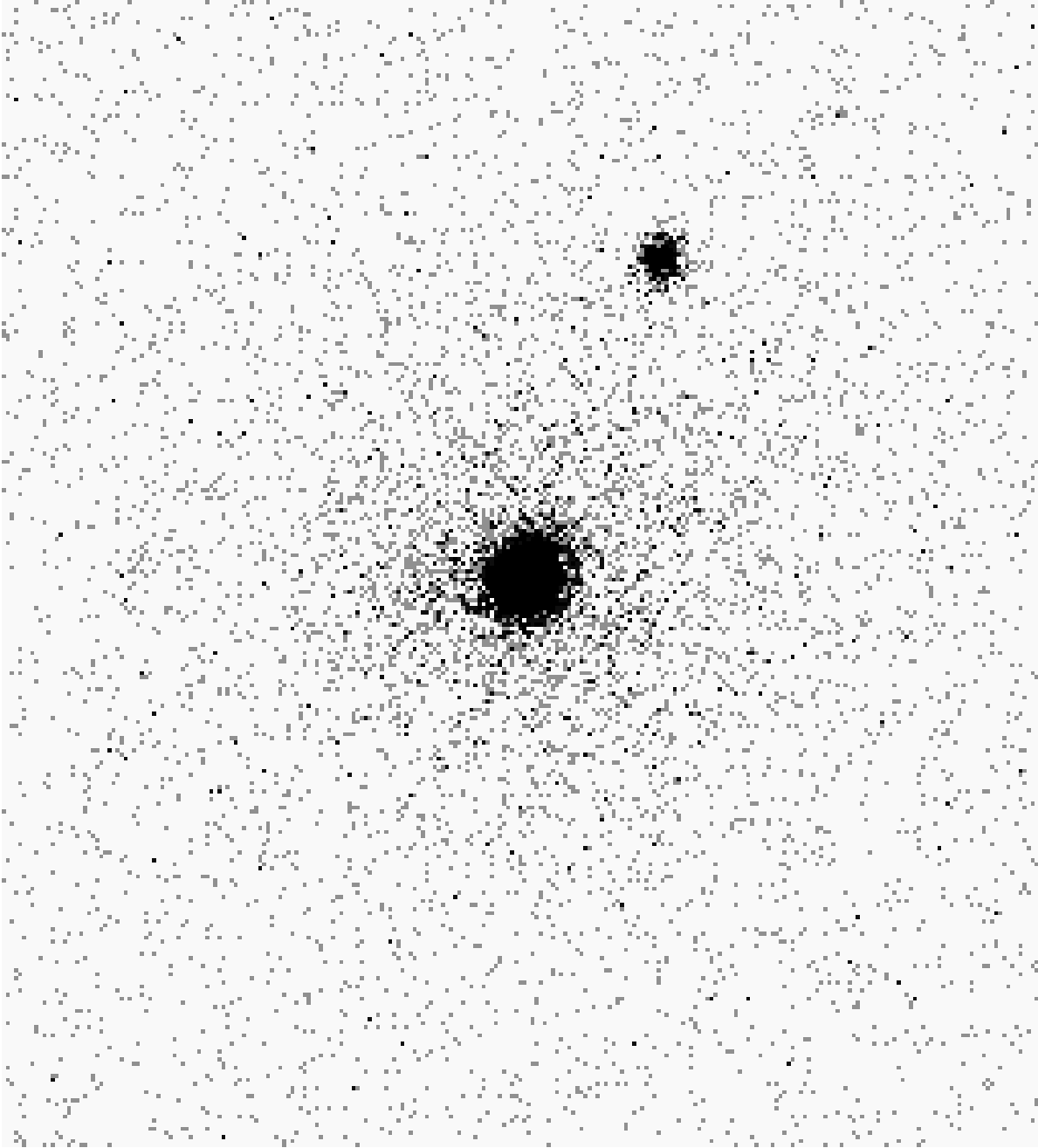


Fig. 2.— The central portion of the *ROSAT* HRI image of the H 1821+643 field. North is up and east is to the left. The image has been binned into  $1''$  pixels but has not been smoothed. The quasar is at the center of the image and the white dwarf is  $88''$  to the NW. The quasar is clearly surrounded by excess emission, above that expected from a point source, from its host cluster.



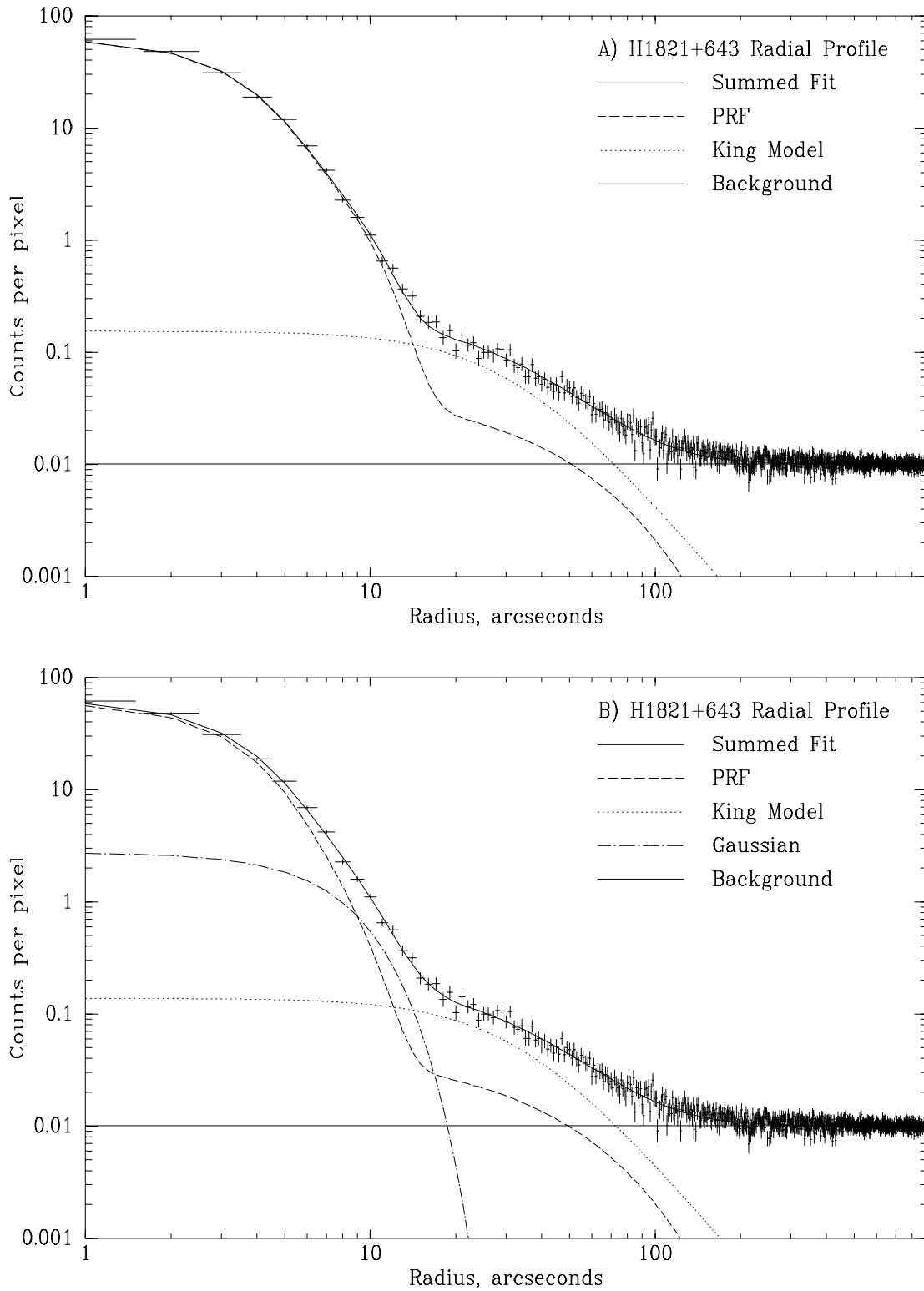


Fig. 3.— Observed radial profile of the quasar H 1821+643 and two fits to it. a. Fit (solid line) includes background (straight solid line), PRF (dashed), and King model (dotted). b. Fit also includes gaussian component (dot-dash).

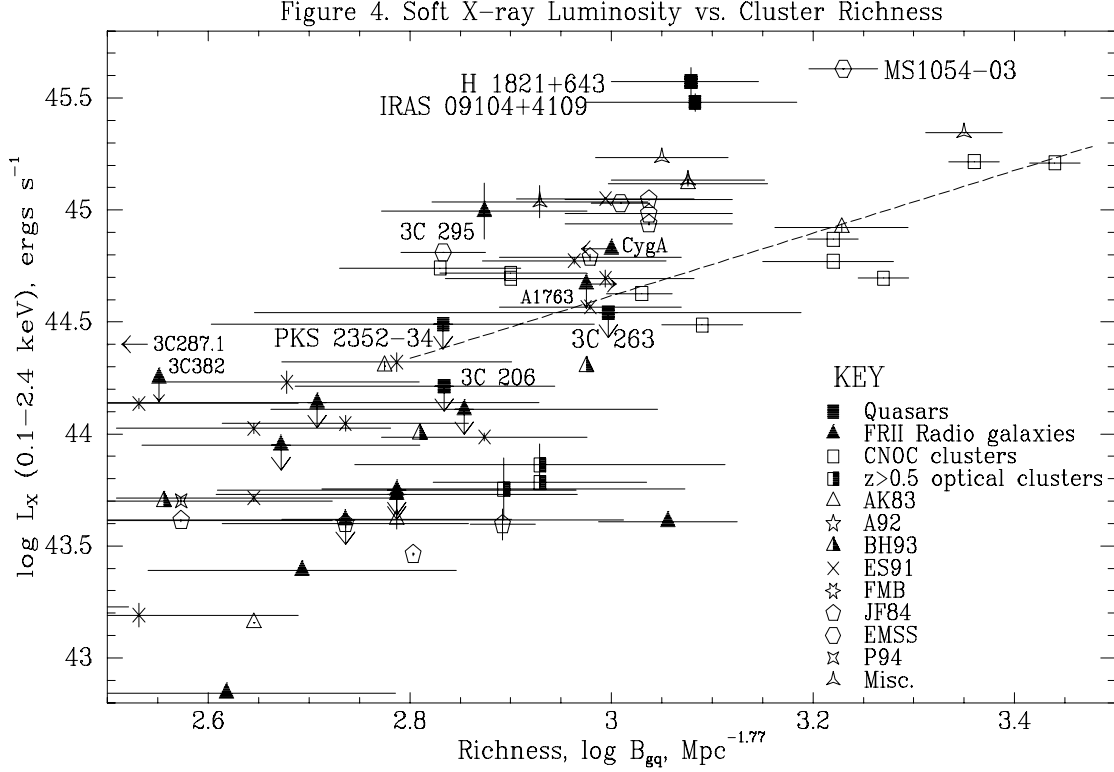


Fig. 4.— The amplitude of the galaxy-cluster center spatial correlation function  $B_{gc}$  vs. rest-frame 0.1-2.4 keV X-ray luminosity  $L_X$ . Quasar host clusters (this work, Paper I, and Fabian & Crawford (1995)) are plotted as filled squares (upper limits assume  $r_{core}=125$  kpc). Open squares are a  $\bar{z}\sim 0.3$  subsample of X-ray selected EMSS clusters being studied by the CNOC group (Carlberg et al. 1996), filled triangles are FR II PRG host clusters, and other symbols are objects from the literature, as detailed in the key. The dotted line is the best fit to the CNOC/EMSS data. Half-filled triangles are typical Abell richness 0, 1, and 2 clusters with  $B_{gc}$  values from EYG91 and  $L_X$  values from Briel & Henry (1993). These  $L_X$  values agree with those from Burg et al. (1994) and Wan & Daly (1996). The typical luminosity for Abell richness 2 clusters falls below the average of objects in our literature dataset, illustrating that said data are extremely inhomogeneous and should be viewed merely as illustrating the range of values observed.  $L_X$  references: Quasars: this work, Paper I, and Fabian & Crawford (1995). PRGs: Henry & Henriksen (1986), Worrall et al. (1994), Crawford & Fabian (1993,1995), O’Dea et al. (1996), and Wan & Daly (1996, and references therein). CNOC/EMSS clusters: Carlberg et al. (1996).  $z>0.5$  optically selected clusters: Castander et al. (1994), Nichol et al. (1994), and Roche et al. (1995). Literature reference keys: AK83: Abramopoulos & Ku (1983); A92: Allen et al. (1992); BH93: Briel & Henry (1993); ES91: Edge & Stewart (1991a,b); FMB: Fabricant, McClintock & Bautz (1991) and Fabricant, Bautz & McClintock (1994); JF84: Jones & Forman (1984); EMSS: Gioia & Luppino (1994), Luppino & Gioia (1995), and Nesci, Perola & Wolter (1994); P94: Pierre et al. (1994a,b); Misc.: Donahue & Stocke (1995); Elbaz, Arnaud & Boehringer (1995); Edge et al. (1994ab); Hughes, Birkinshaw & Huchra (1995); Schwartz et al. (1991); Smail et al. (1995); Schindler et al. (1996); and White et al. (1994).  $B_{gc}$  values taken from (or calculated from  $N_{0.5}$  values given in) Longair & Seldner (1979), Bahcall (1981), Mathieu & Spinrad (1981), Prestage & Peacock (1988), Yates, Miller & Peacock (1989), Hill & Lilly (1991), Allington-Smith et al. (1993), and Yee & Ellingson (1993).

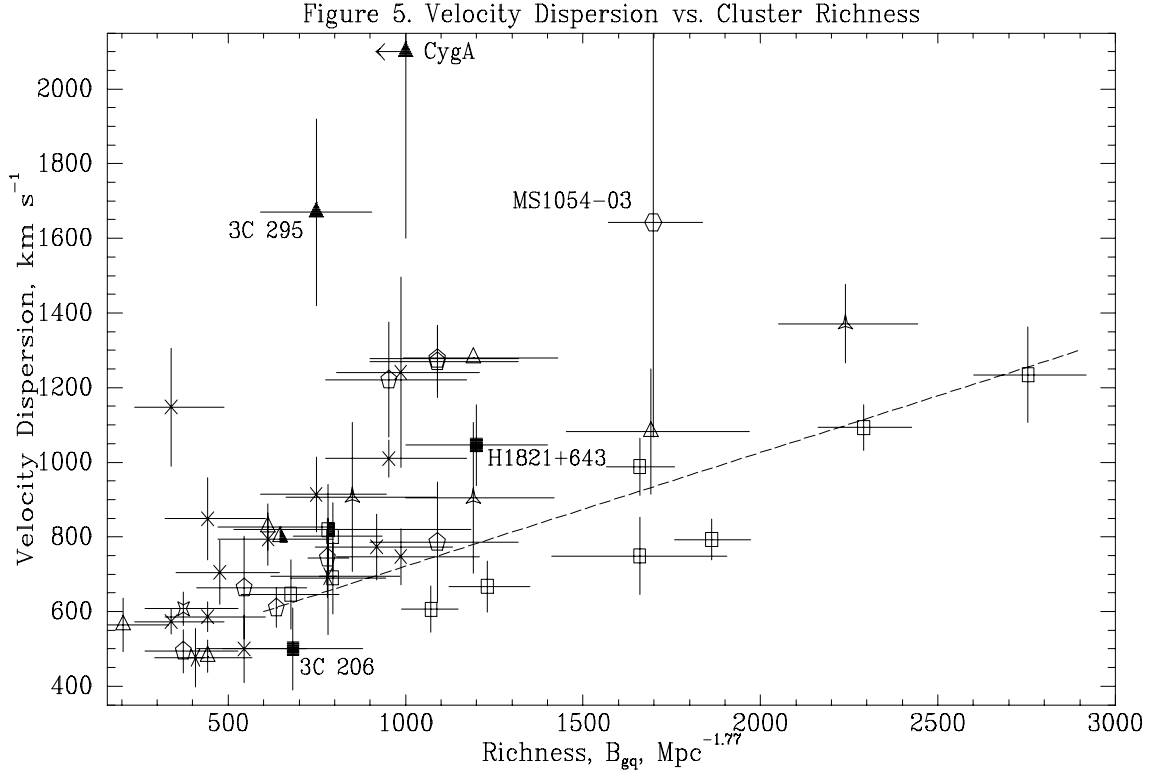


Fig. 5.— Cluster velocity dispersion versus richness. Symbols as in Figure 4. The half-filled triangle is a ‘typical’ Abell richness 1 cluster using  $B_{gq}$  from EYG91 and  $\sigma_v$  from Ellingson, Green & Yee (1991). The half-filled square is CL1322+3027 at  $z=0.757$  (Castander et al. 1994). Velocity dispersions for other literature objects from Struble & Rood (1987), Ellingson et al. (1989), Zabludoff, Huchra & Geller (1990), Teague, Carter & Gray (1990), and Edge & Stewart (1991b).  $B_{gq}$  references are listed in the legend to Figure 4.